Order Number 9432353

Promoter analysis of the *Xenopus laevis* oocyte beta-tubulin gene

Lopingco, Maria Cristina T., Ph.D.

City University of New York, 1994

U·M·I

300 N. Zeeb Rd.
Ann Arbor, MI 48106

PROMOTER ANALYSIS OF THE *XENOPUS LAEVIS* OOCYTE BETA-TUBULIN GENE

by

Maria Cristina T. Lopingco

A dissertation submitted to the Graduate Faculty in Biomedical Sciences in fulfillment of the requirements for the degree of Doctor of Philosophy, the City University of New York

1994

This manuscript has been read and accepted for the Graduate Faculty in Biomedical Sciences in satisfaction of the dissertation requirement for the degree of Doctor of Philosophy.

4/25/94
Date

Chair of Examining Committee

April 25, 1994
Date

Executive Officer

David Bechhofer
James Roberts
Heidi Stuhlmann
Kathleen Scotto
Supervisory Committee

THE CITY UNIVERSITY OF NEW YORK

ABSTRACT

PROMOTER ANALYSIS OF THE *XENOPUS LAEVIS* OOCYTE β-TUBULIN GENE

by

Maria Cristina T. Lopingco

Advisor: James J. Bieker, Ph.D.

The formation of a particular microtubule structure is dictated in part by the ratio of tubulin variants within a cell. This ratio is established by steady-state message levels that are controlled by transcriptional and autoregulatory mechanisms. The *Xenopus laevis* oocyte expresses at least two β-tubulin mRNAs, one (*Xlot*) more abundantly than the other. *Xlot* (**X**enopus laevis **o**ocyte **t**ubulin) is classified as a class IVb β-tubulin based on its tissue distribution and carboxy terminus sequence. It is expressed at low levels in all tissues examined and is upregulated in germ-cells.

A portion of the *Xlot* promoter was cloned and partially sequenced. In addition to the TATA and CAAT boxes, numerous potential cis-elements are present, several of which are also found

in the human class IVb β-tubulin promoter.

The *Xlot* promoter was shown to be capable of driving a significant level of transcription of a reporter gene when microinjected into *Xenopus* oocytes. 336 bp of promoter sequence directly upstream of the transcription start site was characterized by deletion analysis. The minimal promoter is within the first 177 bp. In addition, there are at least 2 regions between nucleotide positions -177 and -336 that modulate minimal promoter activity.

This limited promoter region was divided into the proximal (-121 to +22) and distal (-272 to -116) fragments. Each fragment was shown to form 2 complexes with oocyte proteins. It appears that the protein(s) responsible for complex formation with the proximal and distal fragments are similar, as judged by competition analysis. Potential cis-acting elements identified by sequence comparison of the two fragments were analyzed.

In addition to transcriptional control, oocytes appear to utilize the co-translational autoregulatory mechanism in order to maintain the appropriate level of mRNA. This mechanism requires that the message to be degraded codes for MREI at the amino terminus, and that translation be ongoing beyond residue 41. Message levels are low in oocytes microinjected with constructs encoding tubulin mRNAs with the appropriate signal for autoregulation. When the constructs contain the sequence MVYI at the amino terminus or a stop codon at position nine, steady-state message levels are elevated.

FOR
ESTER

ACKNOWLEDGEMENTS

I would like to thank:

My family - who shall remain nameless lest they fight over the order in which they appear. Thank you for always being there.
Jim Bieker - AHHHHHHHHHHHHHHHHHH my mentor. Thank you for years of care, guidance, patience, encouragement and supply of cheetos.
David Bechhofer and Jim Roberts - for serving on my committee. Thanks for years of baby-sitting.
Terry Krulwich - for putting up with me. Thanks for keeping me out of trouble.
The Yaso woman - thanks for turning me on to chocolate, flowers and DDL. Thanks especially for being such a good friend.
Oscar Weavers - for being such weavas. I'd be lost without you. Thanks for the hours of problem solving and hand-holding. Thank you too for all that curry (and winky company).
Hope-breath - for being uglier than me.
Pinhead and Eileen - for being the best bro and sis-in-law I could hope for.
Members of the Bieker lab, past and present - Mitra Pitra (without whom I wouldn't have a project), Ugly Teppie (for introducing me to terminology one can never find in the Englich language), Ira Jo (for hours of trying to figure out what I did wrong) and Yong (for telling me to "just stop writing").
Chris(sy), Joey and Bederi - thanks for playing with me.
His royal geekness - for making me look normal.
The Ramirez man and members of his lab - thank you for all the advice and reagents. To Ramirez especially, for keeping me skinny by eating all my food.
Hui monster - for introducing me to the world of Mark Morris.
D'aggy and Bekkkkky - thanks for keeping me entertained.
Boaz Gillo - the king of the frogs. Thanks for all the advice.
The gang from Iloilo - thanks for putting up with my absentee-ism.
Micki - without whom I wouldn't be in science. Thanks anyway.
John Styth Pemberton - for inventing COCA-COLA!

TABLE OF CONTENTS

		PAGE
Abstract		iii
Dedication		v
Acknowledgements		vi
Table of Contents		vii
List of Figures		x
List of Tables		xii
CHAPTER 1	INTRODUCTION	1
1.1	Microtubules	1
1.2	Microtubule associated proteins	2
1.3	Post-translational modification of tubulin	3
1.4	Vertebrate tubulin gene families	4
1.5	Sequence comparison of vertebrate β-tubulins	5
1.6	Significance of maintaining several β-tubulin isotypes	7
1.7	Regulation of expression	11
1.8	Transcriptional regulation of β-tubulin	12
1.9	Autoregulatory control of β-tubulin RNA degradation	14
1.10	*Xenopus laevis* family of tubulin genes	16
1.11	*Xenopus laevis* germ-cell β-tubulin	16
1.12	Class IVb β-tubulin	17
1.13	Characteristics of *Xenopus laevis* oocytes	18
1.14	Oocyte β-tubulin protein expression	19
1.15	Oocyte RNA Expression	19
1.16	Oocytes as a system for transcriptional analysis	20
1.17	*Xlot* expression in *Xenopus laevis* oocytes	21
CHAPTER 2	MATERIALS AND METHODS	25
2.1	Bacterial strains	25
2.2	Standard procedures	25
2.3	Mutagenesis with phenotypic selection	26
2.4	Polymerase chain reaction	26
2.5	Constructs for functional analysis	27

2.6	Maintenance of *Xenopus laevis*	28
2.7	Preparation of oocytes for microinjection	28
2.8	Microinjection	29
2.9	RNA isolation and primer extension	29
2.10	Protein isolation and CAT assay	30
2.11	Substrates for *in vitro* analysis	31
2.12	Preparation and purification of total ovary extract	32
2.13	Isolation of oocyte nuclei	33
2.14	Gel mobility-shift assays	33
2.15	DNase protection	34
2.16	Autoregulatory constructs	34
2.17	Purification of erythrocyte and oocyte tubulin	35
2.18	SDS-Polyacrylamide gel electrophoresis	35
2.19	Preparation of antisera against erythroid β-tubulin	35
2.20	Analysis of antisera	36
CHAPTER 3	FUNCTIONAL ANALYSIS OF *Xlot*	37
3.1	Introduction	37
3.2	Results	37
3.2.1	Sequence analysis	37
3.2.2	Identification of substrates for deletion analysis	38
3.2.3	Identification of the aberrant transcript	41
3.2.4	Deletion analysis	42
3.3	Discussion	45
CHAPTER 4	*IN VITRO* ANALYSIS OF TRANS-ACTIVATING FACTORS	65
4.1	Introduction	65
4.2	Results	65
4.2.1	Construction of the proximal and distal fragments	65
4.2.2	Gel-mobility shift assays with total ovary extract	66
4.2.3	Comparison of the fragments' binding activities	67
4.2.4	Analysis of potential cis-acting elements	67
4.2.5	Binding properties of the D1 and D2 complexes	68
4.2.6	DNase I footprint analysis of the distal fragment	69
4.2.7	Binding activity of an oocyte nuclear extract	70
4.2.8	Footprint analysis with nuclear extract	71

4.2.9	Properties of heparin-sepharose purified proteins	71
4.2.10	DNase footprint analysis of pXls11	72
4.3	Discussion	73
CHAPTER 5	CO-TRANSLATIONAL AUTOREGULATION OF β-TUBULIN RNA	88
5.1	Introduction	88
5.2	Results	89
5.3	Discussion	90
CHAPTER 6	*XENOPUS LAEVIS* ERYTHROID β-TUBULIN	
6.1	Introduction	94
6.2	Results	95
6.2.1	cDNA library screening	95
6.2.2	Purification of erythroid and oocyte β-tubulins	96
6.2.3	Generation of polyclonal antibodies	97
6.3	Discussion	97
CHAPTER 7	DISCUSSION	99
CHAPTER 8	BIBLIOGRAPHY	104

LIST OF FIGURES

		PAGE
Figure 1	Summary of cis-acting, tissue-specific elements regulating b3-tubulin gene expression during Drosophila melanogaster embryogenesis	24
Figure 2	Construction of p33B	50
Figure 3	Partial sequence of the 33B genomic fragment	52
Figure 4	Construction of the autoregulatory mutant pSal33B	53
Figure 5	pSal33B-derived transcription in X. laevis oocytes	54
Figure 6	Transcription from a 272 bp promoter	55
Figure 7	Sizing of tubulin RNA derived from microinjected templates	56
Figure 8	Map of pBLCAT6	58
Figure 9	Construction of the "full length" tubulin-CAT fusion, p33BXbal-BglII	59
Figure 10	Construction of promoter deletion mutants	60
Figure 11	CAT activity derived from tubulin-CAT fusion constructs microinjected into oocytes	61
Figure 12	Quantitation of CAT activity from chimeric tubulin-CAT deletion constructs	62
Figure 13	Summary of regulatory regions and potential	64
Figure 14	Construction of the proximal and distal fragments	77
Figure 15	Gel mobility-shift assays of the proximal and distal fragments	78
Figure 16	Competition of the proximal and distal fragments for complex formation	79
Figure 17	Competition for complex formation by the CAAT and AP2 binding sites	80
Figure 18	Kinetic analysis of complex formation	81
Figure 19	A comparison of complex formation by the total ovary extract and nuclear extract	82
Figure 20	Gel-shift/footprint analysis of the distal fragment	83

Figure 21	Gel-mobility shift assays with heparin-sepharose purified oocyte proteins	84
Figure 22	Titration of Poly d(I-C)	85
Figure 23	DNase I footprint analysis of a somatic 5S RNA gene	86
Figure 24	Summary of complex formation	87
Figure 25	Autoregulation of tubulin RNA - 1	92
Figure 26	Autoregulation of tubulin RNA - 2	93
Figure 27	Separation of *Xenopus laevis* oocyte α- and β-tubulins	98

LIST OF TABLES

		PAGE
Table 1	Classification of β-tubulin based on carboxy termini sequence	22
Table 2	Tissue distribution of β-tubulin genes	23

1. INTRODUCTION

1.1 Microtubules

Eukaryotic cells contain dynamic structures that impart a variety of cellular sizes and shapes. These structures also influence subcellular properties such as directional transport and spatial organization of molecules and organelles. These characteristics of morphogenic plasticity and motion are facilitated in part by the workings of microtubules.

Microtubules are filamentous polymers comprised of repeating alpha- and beta-tubulin heterodimers. The α and β polypeptides are globular, soluble and 40-55% similar to each other in amino acid sequence (Ponstingl et al., 1988; Valenzuela et al., 1981). Each monomer has a mass of 55 kDa. Native tubulin *in vivo* exists in the form of soluble α/β heterodimers. Dimers are arranged "head to tail" within a linear protofilament. Thirteen protofilaments are arranged laterally and circularized to form a microtubule, a hollow tube with a diameter of 24-nm. Microtubules are polar organelles wherein both ends of the structure are unequal with respect to polymerization and depolymerization (Engelborghs, 1990). The "plus" end is more active in assembly while the "minus" end disassembles more rapidly. Furthermore, the minus ends are inserted into microtubule organising centers (centrosomes). A divergent tubulin called gamma tubulin has also been identified. Unlike α- and β-, γ-tubulin does not occur in significant amounts within microtubule polymers, but is associated with microtubule organizing centers (Oakley and Oakley, 1989; Oakley et al., 1990; Stearns et al., 1991; Zheng et al., 1991).

Microtubules form a large and varied collection of subcellular structures capable of performing a wide range of functions. These include: flagellar motility, axoplasmic flow, chromosome segregation, intracellular transport/organelle localization, secretion, and in concert with micro- and intermediate filaments, form the internal cytoarchitecture. Microtubules form either permanent or transient structures within a cell. For example, the cytoskeletal lattice that extends along neuronal axons and dendrites has a lifetime of over 100 days. On the other hand, the microtubule network of interphase cells is disassembled with each mitotic event. The released tubulin heterodimers reassemble, forming the mitotic spindle responsible for partitioning chromosomes between daughter cells.

Since microtubules are constructed from repeating subunits, diversification is necessary in order to form the versatile structures discussed above. Diversification is achieved in several ways. First, microtubules are associated with accessory proteins collectively termed microtubule associated proteins (MAPs). Second, microtubules can be post-translationally modified. Finally, the α- and β-tubulin proteins are encoded for by gene families whose members' expression are individually controlled by each cell type.

1.2 Microtubule associated proteins

Microtubule associated proteins (MAPs) are classified into three broad categories. These are fibrous MAPs, energy-transducing MAPs, and non-fibrous MAPs.

Fibrous MAPs function in microtubule crosslinking, influencing polymer stability (Drubin and Kirschner, 1986). They

also control the spacing between parallel microtubules or between microtubules and other cytoskeletal elements (Neve et al., 1986; Binder et al., 1985). Energy-transducing MAPs function primarily in microtubule-dependent motility and organelle transport (Gelles et al., 1988). A second function is the maintenance of the dynamic structure of intracellular membrane networks such as the endoplasmic reticulum (Dabora and Sheetz, 1988; Vale and Hotani, 1988). The final MAP category consists of non-fibrous MAPs whose functions are not clearly defined. Members of this group have been proposed to play a role in spindle formation and stabilization of microtubules (Hirokawa et al., 1985; Feick et al., 1991).

1.3 *Post-translational modification of tubulin*

Post-translational modifications probably provide chemical signals on the microtubule surface, designating them towards a specific subcellular locale or structure. Tubulin proteins are subject to acetylation, tyrosylation/detyrosylation, phosphorylation and glutamylation.

(De)tyrosylation is possible in α-tubulins with a tyrosine as the carboxy terminal residue. Microtubules formed from detyrosylated tubulin have been colocalized with the golgi apparatus (Skoufias et al., 1990). Acetylation occurs on α-tubulin (Schibler and Huang, 1991). Detyrosylated and acetylated tubulins are associated with microtubules resistant to depolymerization by anti-mitotic drugs (Piperno et al., 1987; Gundersen and Bulinskik 1986). Phosphorylation is restricted to the minor neuronal β-tubulin (Alexander et al., 1991; Table II, Class III). Finally, addition of 3-6 glutamic acid molecules occurs in a class III β-tubulin and an undetermined number of α-

tubulins (Alexander et al., 1991; Edde et al., 1990).

1.4 Vertebrate tubulin gene families

A third means by which microtubule diversity can be achieved is by the developmental and tissue specific expression of different members of the α- and β-tubulin superfamilies of genes. The most extensive data on α-tubulin comes from mice where at least seven genes encode six polypeptide isotypes (Villasante et al., 1986; Hecht et al., 1988). Five functional genes have been identified in chickens (Valenzuela et al., 1981; Pratt et al., 1987; Pratt and Cleveland, 1988). The remainder of this discussion will focus on the β-tubulin gene family, except where noted.

The majority of vertebrate β-tubulin genes consist of four exons interrupted by three introns at characteristic nucleotide positions (Sullivan et al., 1986b). All encoded proteins display a conserved amino acid framework between residues 1 and 430. The carboxy termini, beyond residue 430, are 14-21 amino acids in length. Six types of carboxy terminal sequences define all vertebrate β-tubulins (Table I; Sullivan and Cleveland, 1986).

Expression of the six β-tubulin isotypic classes is highly conserved, each isoform synthesized in similar tissues across species (Table II). Class I is an abundant, ubiquitously expressed isotype. Class II is also found in many tissues but largely in the brain. It is associated with neuronal regeneration and development (Hoffman and Cleveland, 1988). Class III is a minor neuronal polypeptide found in the brain and dorsal root ganglia of chordates (Little and Luduena, 1985; Sullivan et al., 1984; Luduena et al., 1982). Its expression increases during axonal

outgrowth (Burgoyne et al., 1988; Joshi and Cleveland, 1989; Moskowitz et al., 1993). This isotype appears in differentiated cells but not in mitotic neuroblasts (Lee et al., 1989). There are exceptions to this expression pattern, however. Class III β-tubulin is also found in testicular sertoli cells (Lewis and Cowan, 1988) as well as in certain tumors of non-neural origin but only after their transformation (Matsuzaki et al., 1987; Scott et al., 1990). Class IV genes are divided into 2 groups based on expression pattern. Class IVa β-tubulin is abundant in neural tissue in later stages of development. Class IVb is the major germ cell β-tubulin which is in addition constitutively expressed in a variety of tissues (Hoffman and Cleveland, 1988; Sullivan et al., 1986; Bieker and Yazdani-Buicky, 1992). Only chickens have been examined for Class V expression. The protein is absent from neurons but is otherwise expressed ubiquitously as well as in certain cultured mammalian cells (Sullivan et al., 1986a; Lopata and Cleveland, 1987; Ahmad et al., 1991). Class VI β-tubulin is restricted to erythroid cells where it forms the marginal band (Murphy et al., 1987; Wang et al., 1986).

1.5 Sequence comparison of vertebrate β-tubulins

Inter- and intra-species comparisons of β-tubulin protein sequences show a high degree of homology. The mouse erythroid isovariant, the most divergent, is at least 77% similar to all other vertebrate β-tubulins. The chicken counterpart shows at least 81% homology (excluding the mouse isoform). If the hematopoietic tubulins are not taken into account, sequence similarity is greater than 90% intra- and inter-species (Little and Seehaus, 1988).

While tubulin proteins show a generally conserved amino

acid framework, there are specific regions of absolute homology and heterogeneity. The first region of conservation is between amino acids 384-426, a region of yet undefined function. Conservation is also observed at positions 58-67, 140-146, 178-181 and 240-244. These last four regions are proposed to be GTP binding sites (Linse and Mandelkow, 1988).

The carboxy terminus as well as amino acids 30-57 and 68-100 represent the regions of non-homology. The carboxy termini can be considered conserved since only six sequences represent all β-tubulins. However, they have generally been classified as "highly variable" because a comparison of all six sequences does not reveal an obvious similarity among them, similar to the homology of the first 430 amino acids observed among all β-tubulins. These termini are glutamate-rich, therefore highly negatively charged. It has been suggested that these negative charges inhibit microtubule assembly (Mejillano and Himes, 1991). *In vivo*, inhibition is relieved by MAP binding (Littauer et al., 1986) whereas removal of these regions permits polymerization in the absence of MAPs (Serrano et al., 1984). A second region of lesser heterogeneity is roughly between residues 30 and 100 (Sullivan and Cleveland, 1986). Three "hot spots" that partially overlap this region have been identified (Burns and Surridge, 1990). Like the carboxy termini, these "hot spots" vary between the six isotypes but are conserved within each class, inter-species. Hot spots are located at residues 35, 55-57 and 124, and have several notable characteristics: 1) a change at one site is always accompanied by coordinated changes at the two other sites, 2) the same substitutions are found in all beta-tubulins of the same class, however, 3) similar substitutions may

occur in more than one class. The authors further propose that the three "hot spots" interact with the C-terminus, which in turn interacts with residues 217/218. The interactions may be involved in effecting the conformational change induced by the assembly dependent GTP hydrolysis which is responsible for dynamic instability, the elongation and shortening phases of microtubules (Carlier et al., 1984).

1.6 Significance of maintaining several β-tubulin isotypes

β-tubulin protein sequences are highly homologous and the microtubules they form show conserved inter-species ultrastructure (Valenzuela et al., 1981). Because of such conservation, the existence of 6 isotypes is quite perplexing.

Two hypotheses have been put forward to explain the necessity of a gene family. The "isotubulin hypothesis" proposes that the various tubulins are functionally equivalent. The gene family evolved in order to regulate the amount of tubulin protein in different cell types and during alternative programs of development and differentiation. This is accomplished by having six different promoters (Raff, 1984; Raff et al., 1987). The "multi-tubulin" hypothesis suggests that the various tubulin polypeptides have different functional properties, each tailored to particular applications within various cells (Fulton and Simpson, 1976). There is extensive evidence in support of both hypotheses

The isotubulin hypothesis is supported by data showing: 1) Identical proteins are expressed in different tissues. The chicken cβ1 and cβ2 products vary by two conservative amino acid

substitutions. The coding and 5' flanking sequences are 99.1% and 80% identical, respectively. Both transcripts are detected at low levels in many cell types. However, cβ1 is the predominant β-tubulin gene expressed in cultured skeletal myoblasts and cβ2 is abundant in neural cells (Sullivan et al., 1984). This argues that isotypes evolved to regulate expression in different tissues; and 2) Heterologous tubulins are copolymerized or reconstituted into microtubules. In cultured cells, microtubule structures such as the interphase cytoplasmic array, spindle and midbody microtubules, are assembled from copolymers of all available isotypes. There is no preferential utilization of a specific isotype by any one structure (Lopata and Cleveland, 1987; Ahmad et al., 1991). A heterologous isovariant, normally restricted to mouse fetal erythroblasts and mature megakaryocytes, is efficiently assembled into both cytoplasmic and spindle microtubules of Hela cells (Lewis et al., 1987). Likewise, the chicken erythroid variant is competent for assembly into divergent microtubule structures (Joshi et al., 1987). Conversely, Swan and Solomon (1984) recapitulated the erythroid marginal band using purified brain tubulin (devoid of MAPs), which alone is assembly-incompetent. Thus, it appears that the erythrocyte milieu contains the necessary components to direct formation of the marginal band structure. The most striking evidence in support of this theory comes from studies involving chimeric tubulin. Mouse 3T3 cells were transfected with a tubulin gene containing a chicken 5' end similar but not identical to the mouse proteins, and a highly divergent yeast 3' end. The chimeric tubulin behaved indistinguishably from endogenous β-tubulins (Bond et al., 1986).

The rationale for introducing variant tubulin sequences is

that the inappropriate protein, if functionally significant, would disrupt some cell function or produce a distinct intracellular distribution of microtubles. While the studies presented above indicate a lack of functional significance the following caveat is offered. In the above mentioned transfection experiments of Lewis et al. (1987) and Bond et al. (1986), the variant isotypes were produced at $\leq$10% of total tubulin. It is arguable that these levels are not sufficient to induce functional aberration.

A second set of studies supports the multi-tubulin hypothesis. This includes: 1) evolutionary analysis; 2) conservation of functionally significant regions; 3) preferential utilization of isotypes; and 4) mutations that affect function. Evolutionary analysis shows that divergence of the six vertebrate classes started 450 million years ago and was completed over 280 million years ago. Because the variable regions have since been conserved, they must offer a selective advantage and are functionally significant. For example, post-translational modifications and binding to certain MAPs, responsible for microtubule diversity, are controlled by the "variable" carboxy terminal sequence (Littauer et al. 1986; Cross 1991). In addition, the region between positions 28-38 shows variation among, but conservation within isotypes, and has been observed to be involved in tubulin-tubulin interactions (Chene et al., 1992). Finally, sulfhydryl groups have been proposed to regulate microtubule assembly (Luduena and Roach, 1991). The most divergent class VI proteins have one or two cysteines in this area and disulfide bonds have been observed in platelets, but not in other forms of tubulin structures (Ikeda and Steiner, 1978). In summary, the interactions dictated by the variable regions

influence the properties of the resulting microtubule structure.

Working under the assumption that varying isotype characteristics facilitates the formation of varied microtubule structures, segregation of isotype subsets by microtubule structure is expected. In cultured neuronal cells (Falconer et al., 1992) and pheochromocytoma cells (Asai and Remolona, 1989), there is preferential incorporation of class II and class III β-tubulin into colchicine stable and labile structures, respectively. Rat PC-12 cells express five β-tubulin isotypes. In general, there is a greater use of class I and II, and underassembly of classes III and IV isotypes in microtubule structures. Class V is preferentially excluded from neurites (Joshi and Cleveland,1989). Bovine retinal rod cells and tracheal cilia both express class II and class IV tubulins. However, non-axonemal and axonemal microtubules preferentially contain class V and IV respectively (Renthal et al., 1993).

The most notable argument for functional significance of beta tubulin isotypes comes from studies on *Drosophila melanogaster.* Different mutations within the testis-specific β2 structural region affect different functions. For example in $\beta 2t^7$ and $\beta 2t^8$ mutants, cytokinesis is disrupted and axonemes are irregular. However, $\beta 2t^7$ supports nuclear elongation and chromosome movement, whereas no nuclear shaping occurs in $\beta 2t^8$ mutants. In addition, sister chromatids separate but remain scattered across the spindle in $\beta 2t^8$ mutants (Fuller et al., 1988). Thus, not only do isotypes vary in function, regions within isotypes vary as well.

It appears that both theories are valid. Cells regulate the ratio of various isotypes. Some isotypes have a global role, while others facilitate specific interactions. Thus, the characteristics

of the final microtubule structure may depend on the proportion of each isotype. The importance of isotype proportion is underscored by the "threshold effect" phenomenon. When *Drosophila* β2 is replaced with β3, certain functions such as mitochondrial elongation occur normally. However, meiosis, nuclear shaping and axoneme formation are severely compromised. If both β2 and β3 are expressed, then male sterility is observed when β3 exceeds 20% of total tubulin. In these flies, axoneme formation is disrupted (Hoyle and Raff, 1990). In addition to the Drosophila example above, this phenomenon has also been demonstrated for PtK_2 cells. Microtubule stability is affected only when microinjected *Physarum* tubulin exceeds a critical percentage (Prescott et al.,1989).

1.7 Regulation of expression

Isotype expression varies depending on the need for certain microtubule structures throughout development, as well as in different cell types. For example, the ratio of cβ1 to cβ2 RNA levels are 1.6, 7.3 and 0.10 in chicken fibroblast, myoblasts and neurons respectively. This is due to a large difference in the level of cβ2 (Sullivan et al., 1985). The level of late neural tubulin RNA increases at birth, peaks by day 21, then decreases and is maintained at a level lower than at the first day (Wagner et al., 1992). In differentiating neurons, such as PC12 cells, class I, II and III proteins increase while the expression of class IV and V remain unchanged (Joshi and Cleveland, 1989).

The differential isotype responsiveness could be partially attributed to a change in trans-activating factor availability.

Hela cell β-tubulin transcription is stimulated 2-6 fold during the early stages of adenovirus infection. Transcription is dependent on the trans-acting factor E1a, and follows the response kinetics of the E1a-dependent E3 gene. This is not a general phenomenon as beta-actin is not upregulated and beta-globin is still not transcribed (Stein and Ziff, 1984).

1.8 Transcriptional regulation of β-tubulin

Vertebrate tubulin promoters have not been analyzed. However, some advances have been made in non-vertebrates. The most complex organism whose tubulin promoters have been dissected is *Drosophila*.

The four *Drosophila* β-tubulins, which are divided into three classes, are expressed in a developmental and tissue specific manner (Bialojan et al.,1984; Natzle and McCarthy, 1984; Gasch et al., 1988; Leiss et al., 1988; Michiels et al., 1987; Rudolph et al., 1987). β1 tubulin is the predominant isotype in all tissues except the testis, where it is dominant in premeiotic cells only (Natzle and McCarthy, 1984; Rudolph et al., 1987). Transcription in nurse cells of the egg chamber and upregulation in neural derivatives is dependent on an enhancer-like intron in cooperation with upstream sequences (Buttgereit et al., 1990). β2 is testis specific, functioning in spermatocyte differentiation into motile spermatozoa (Rudolph et al., 1987). The regulatory region is remarkably simple. First, a correctly positioned 14-bp element (β2UE1), is necessary and sufficient for testis specific expression. A second element is present at nucleotide positions -32 to -26. While not responsible for tissue specificity, this second element performs a quantitative function, influencing the

level of transcription (Michiels et al., 1989).

Highest levels of β3 expression are restricted to two phases: mid-embryogenesis and metamorphosis. However, it is also a minor and transient component of several tissues. Transcriptional activation in various mesodermal derivatives during mid-embryogenesis requires distinct though redundant cis-acting elements. At least one element upstream of nucleotide -1200 mediates expression in somatic and pharyngeal muscles, and the dorsal vessel (Figure 1, sm1). The 4.5 kb first intron is enhancer-like, activating transcription in a distance-independent manner (Gasch et al., 1989). A 334 bp region within this intron together with 230 bp of 5' upstream flanking sequence regulates expression in the entire visceral musculature at stage 11 and somatic mesoderm at stage 14 (Figure 1, vm2 and sm3). An adjacent intronic region additionally facilitates β3 transcription in the abdominal region of the visceral musculature and in a subset of somatic muscles (Figure 1, vm1 and sm2) (Hinz et al., 1992).

Several factors have been proposed to regulate β3 transcription. First, the transcription factor *Ubx* (White and Wilcox, 1985) or a *Ubx*-dependent factor partially controls the activity of vm1 (Hinz et al., 1992). Second, a decline in *twist* expression (Thisse et al., 1988) correlates with the activation of β3 tubulin synthesis although the exact nature of this regulation has not been determined (Currie and Bate, 1991). Finally, β3 tubulin is regulated by the hormonal steroid 20-hydroxyecdysone (20-OH-E) (Sobrier et al., 1989). In *Drosophila* Kc cells, 910 bp of upstream flanking sequence alone contains hormone-independent positive element(s). Addition of the terminal 500 bp of intron 1 represses the activity of this upstream sequence in

the absence of hormone. Addition of 20-OH-E not only relieves the repression but additionally stimulates transcription, above the level dictated by the upstream sequence (Bruhat et al., 1990).

1.9 Autoregulatory control of β-tubulin RNA degradation

Autoregulation represents a second mechanism, in addition to transcriptional control, that regulates the level and ratio of tubulin RNA, therefore the level of tubulin protein. Tubulin protein synthesis is modulated by the level of unpolymerized tubulin subunits. Ben Ze'ev et al. (1979), were the first to report repression of α– and β-tubulin protein synthesis when the intracellular level of free tubulin subunits is raised by microtubule depolymerization. However, when depolymerization is followed by tubulin precipitation, tubulin protein synthesis is specifically enhanced.

Repression of protein synthesis results from a decrease in the level of cytoplasmic RNA (Cleveland et al., 1981). This is established in the cytoplasm since the level of newly transcribed tubulin RNA from nuclei of microtubule-depolymerized cells is similar to that from untreated cells. However, <10% of tubulin RNA is left in the postnuclear extract only of cells treated with a depolymerizing agent compared to untreated cells (Cleveland and Havercroft, 1983). Additionally, substitution of the tubulin promoter with a metallothionein promoter does not disrupt autoregulation (Gay et al., 1987). Finally, significant depression in β-tubulin protein synthesis occurs in microtubule-depolymerized enucleated cells compared to control cytoplasts. These studies demonstrate that the decrease in tubulin RNA level is not due to a down-regulation of transcription.

The first 13 nucleotides of tubulin RNA contain the signal for autoregulation (Gay et al., 1987). However, the translated amino acids, not the RNA, are what bring about RNA degradation. For example, transcripts with an altered mRNA, but not polypeptide, sequence are still substrates for autoregulation. On the protein level, the sequence Methionine-Arginine-Glutamine-Isoleucine (MREI) is sufficient and required to be at the amino terminus, since autoregulation is abolished when this region is internalized. Of all known protein sequences, only β-tubulins have MREI at their amino terminus. Autoregulatable α-tubulins begin with MRE (Yen et al., 1988b)

Tubulin polypeptide promotes RNA degradation only when the corresponding RNA is polysome bound and is in the process of being translated beyond codon 41. A ribosome covers approximately 30-40 amino acids, and translation beyond this number is necessary for the first four amino acids to emerge (Yen et al., 1988a). Treatment with agents that promote mRNA release from the ribosome or translation termination prior to amino acid 42 both disrupt autoregulation (Pachter et al., 1987; Gay et al., 1989).

There is evidence that a cellular factor binds to the nascent β-tubulin peptide, marking its associated RNA as a substrate for degradation. While the expected candidate for this factor is tubulin, purified tubulin does not bind to a synthetic peptide corresponding to the 12 amino terminal residues of tubulin. However, injection of a monoclonal antibody raised against the same synthetic peptide successfully abolishes autoregulation. These findings suggest that antibody binding prevents binding of an, as yet, uncharacterized factor. This effect is β-tubulin-specific since α-tubulin is not degraded (Theodorakis and

Cleveland, 1992).

1.10 *Xenopus laevis* family of tubulin genes

Xenopus laevis or African clawed frog, encodes a family of at least three β-tubulin genes (Bieker and Yazdani-Buicky, 1992), two of which have been isolated. The neural isotype is not maternally expressed, as its RNA is not detected in eggs. RNA accumulation commences in the nervous system in early gastrula (stage 11) (Richter et al., 1988; Dworkin-Rastl et al., 1986). This isotype is classified as a class II β-tubulin based on its C-terminal sequence and tissue distribution (Good et al., 1988; Sullivan and Cleveland, 1986). The second gene, *Xlot* (*Xenopus laevis* oocyte tubulin), is discussed in detail below.

1.11 *Xenopus laevis* germ-cell β-tubulin

The *X. laevis* germ-cell β-tubulin, *Xlot*, is a class IVb member based on its carboxy terminal sequence and tissue distribution. The unusual polyadenylation signal ATTAA shared by the chicken and mouse class IVb tubulins (Bieker and Yazdani-Buicky, 1992; Sullivan et al., 1986a; Wang et al., 1986) is found at nucleotide 1516 in the cDNA. The encoded 445 amino acid polypeptide is initiated at +60 of the mRNA.

Xlot is expressed in a wide range of tissues, the highest levels being primarily in testis and secondarily in oocytes. Within the ovary, steady state levels of *Xlot* RNA are highest in immature oocytes and decrease six-fold by stage V/VI (Bieker and Yazdani-Buicky, 1992; Pestell, 1975; section 1.13). The decrease in RNA levels is in accordance with the autoregulatory mechanism discussed above, since soluble tubulin protein

concentrations are lowest in immature oocytes and highest in late stage oocytes (Pestell, 1975). *Xlot* message levels increase no more than two-fold upon maturation of stage VI oocytes into eggs. This can again be explained by autoregulation, since the formation of the mitotic spindle lowers soluble heterodimer levels. During embryogenesis, steady state RNA level is maintained at a constant amount per embryo despite a large increase in the number of cells per embryo (Bieker and Yazdani-Buicky, 1992). This is in contrast to actin, another cytoskeletal component, whose message levels increase with cell number (Mohun et al., 1984).

Xlot RNA is initiated at four start sites: +1 (major start site in oocytes), -1, -3 and -4. Start site utilization changes throughout germ-line formation and embryogenesis. The pattern is as follows: 1) stage I-IV oocytes (all sites), 2) stage V/VI oocytes and embryos until gastrulation (+1), 3) embryos in late gastrula (+1 and -1) and 4) stage 40 embryos (all sites) (Bieker and Yazdani-Buicky, 1992). Multiple start site utilization at stage 40 precedes the appearance of primordial germ cells in the indifferent gonad at stage 45 (Al-Mukhtar and Webb, 1971; Holwill et al., 1987). This start site utilization phenomenon is common to numerous β- and α-tubulins (Havercroft and Cleveland, 1984; Wang et al., 1986; Lewis et al., 1985; Sullivan et al., 1985; Middleton and Morgan, 1989).

1.12 Class IVb β-tubulin

Class IVb tubulins have also been isolated from humans, mice and chickens. Human hβ2 has been detected in squamous cell carcinoma, epithelial cells and an embryonic kidney cell line

(Lewis et al., 1985). Classification is based on its carboxy terminal sequence. Mouse mβ3 is expressed at low levels in various post-natal tissues including testis. Testis expression increases by day 32 to 10-20 fold the levels in other tissues. Brain expression is significantly lower (Wang et al., 1986). Chicken cβ3 is detected at a constant, low level in total RNA from day 3-12 embryos. In adult tissues expression is ubiquitous but highest in testis. Interestingly, the ubiquitous cβ2 (class II), is more pronounced than cβ3 in all embryonic cells except primitive red blood cells. In adult tissues excluding brain and lung, cβ3 is more prominent than cβ2 (Havercroft and Cleveland, 1984).

1.13 Characteristics of *Xenopus laevis* oocytes

The *Xenopus laevis* ovary consists of a string of oocytes enveloped by two epithelial and one follicular cell layers, and each adult ovary is divided into 24 lobes (Dumont, 1972). Oogenesis is both continuous, with oocytes formed from a dividing stem cell population called oogonia, and asynchronous, each ovary containing oocytes in all stages of development.

There are six morphological stages of development as characterized by Dumont (1972). What follows is a brief description of the six stages. Transparent stage I oocytes are previtellogenic and range from 50-300 μm in diameter. Vitellogenesis, or the synthesis and uptake of yolk, begins at stage II, pigmentation appears at stage III, accumulation of pigment in the animal hemisphere at stage IV, and displacement of the nucleus towards the animal pole at stage V. The 1200 to 1300-μm-diameter stage VI oocytes are post-vitellogenic and are best characterized by an unpigmented equatorial band between the animal and vegetal pole. Their nuclei are 10^5 times larger

than those in somatic cells. The large size of stage V/VI oocytes and their nuclei makes them ideal for microinjection. Stage V and VI oocytes comprise 10% and 17% of a stage II-VI population, respectively. Development from stage I to VI takes at least eight months with progression through the stages being variable in time (Gurdon and Wickens, 1983).

1.14 Oocyte β-tubulin protein expression

Protein synthesis increases 100-fold throughout oocyte development such that by stage VI, 400 ng protein is produced daily. Stage VI oocytes contain 0.4 μg of total tubulin heterodimer of which only 19-25% is polymerized (Jessus et al., 1987; Gard and Kirschner, 1987). The low level of assembly is most likely due to the lack of co-factors such as MAPs (Heidemann et al., 1985). Microtubules that do form appear to play a crucial role in the establishment of the initial animal-vegetal axis (Gard, 1991) and have been implicated in the localization of subcellular organelles and maternal mRNAs such as Vg1 (Yisraeli et al., 1990).

1.15 Oocyte RNA Expression

There are 10^5 times more RNA polymerase molecules in an oocyte than in a somatic cell, with equal activities of polymerases I, II and III (Roeder, 1974). Since polymerase molecules are only 100-200 nucleotides apart on the chromosome, transcription is at a maximum, 20 ng/day (Miller and Bakken, 1972; Hill, 1979). Stage VI oocytes contain approximately five micrograms of total RNA, the majority of which is ribosomal.

By stage VI, an oocyte contains 80-90 ng of total Poly A^+ RNA (Dolecki and Smith, 1979; Sagata et al., 1980) of which 78% is cytoplasmic. This represents 4 x 10^6 copies of each maternal RNA encoded by 1-2 x 10^4 different genes (Davidson, 1986). Of the total Poly A^+ RNA, 55 ng is non-translatable (transcripts containing repetitive elements within), 13.5 ng is mitochondrial and 21.5 is translatable (Anderson et al., 1982; Richter et al., 1984; Webb et al., 1977; Dolecki and Smith, 1979). The final level of translatable cytoplasmic Poly A^+ RNA is reached before the end of stage II (Golden et al., 1980). Transcription nevertheless remains maximal throughout oogenesis with the level of cytoplasmic Poly A^+ RNA maintained by the balance between synthesis and turnover (Davidson, 1986).

1.16 Oocytes as a system for transcriptional analysis

Gene expression can be studied: 1) in cell free systems; 2) by infecting cells with genetically manipulated viruses; 3) by transfecting DNA into cultured cells; or 4) by microinjection into a variety of cells. Microinjection into *Xenopus laevis* oocytes has a number of advantages: 1) Large quantities of oocytes are easily obtainable; 2) Oocytes are large and manipulations such as microinjection can be accomplished with the aid of only a light microscope; 3) Nuclear injection results in a high efficiency transfer of exogenous DNA. The limitation with methods such as transfection is that only a small number of cells take up DNA; 4) *Xenopus* oocytes are extremely active in protein synthesis and transcription because they contain 10^4-10^5 times more ribosomes, histones, RNA polymerases and ribonucleotide triphosphates than a somatic cell. Thus only a small amount of DNA is needed to obtain detectable transcription which, in

addition, can be monitored within a few hours of injection; 5) Injected DNA is not integrated into the host chromosome but is assembled into normal chromatin structure such that expression is not influenced by flanking host sequences; 6) Oocytes are non-dividing cells, inactive with respect to DNA synthesis therefore the DNA sequence is less likely modified; and 7) Injection allows introduction of any cellular component facilitating analysis of trans-acting factors. This obviates the need for expression of such a factor, which itself could be regulated.

1.17 *Xlot* expression in *Xenopus laevis* oocytes

We have investigated the expression of the class IVb β-tubulin, *Xlot*. We are interested in: 1) Identifying cis-acting elements and trans-activating factors responsible for *Xlot* upregulation in Xenopus oocytes. To this end, we have isolated and partially sequenced a genomic fragment containing at least some promoter sequences. By deletion analysis, regions of functional significance have been mapped. Binding activity of oocyte proteins to these regions have also been identified; and 2) Identifying factors within the oocyte milieu responsible for autoregulation. We have initiated studies to determine whether *Xlot* is autoregulated and whether the oocyte system is ideal for dissecting the autoregulatory pathway.

Table 1. Classification of β-tubulin based on carboxy termini sequence.

Six carboxy termini sequences define all vertebrate β-tubulins. The one letter amino acid code shows the extreme carboxy terminal sequences of known vertebrate β-tubulins. Minor heterogeneity within a class are indicated. The erythroid tubulins (class VI) do not show carboxy terminal homology and are grouped as such.

Class I	EEEEDFDEEAEEEA
Class II	DEQGEFEEEGEEDEA EG
Class III	EEEGEMYEDDEEESEGAK SQGPK
Class IVa	EEGEFEEEAEEEVA
Class IVb	EEEGEFEEEAEEEAE VA F ENA
Class V	NDGEEEAFEDDEEEI NE
Class VI	DVEEYEEAEASPEKET GLEDSEEDAEEAEVEAEDKDH

Table 2. Tissue distribution of β-tubulin genes. β-tubulin classification is based on the carboxy terminal sequence (table 1). Tissue distribution is conserved inter-species within a class, as shown below. Several genes are listed and abbreviations are as follows: c (chicken), m (mouse), r (rabbit), h (human), porc. (porcine), bov. (bovine), and X (*Xenopus laevis*).

CLASS	DISTRIBUTION	BETA-TUBULIN
Class I	constitutive many tissues	cβ7, mβ5, rβt.3, hβ1
Class II	major neuronal many tissues	cβ2, mβ2, rβt.1, porc.βA, bov.β1
	skeletal muscle	cβ1
Class III	minor neuronal	cβ4, hβ4, porc.βB, bov.β2
	neuron specific	
Class IVa	major neural brain specific	mβ4, rβt.2, hβ5
Class IVb	major testis many tissues	cβ3, mβ3, hβ2, **Xlot**
Class V	minor constitutive absent from neurons	cβ5
Class VI	erythroid specific	cβ6, mβ1

Figure 1. Summary of cis-acting, tissue-specific elements regulating β3 tubulin gene expression during *Drosophila melanogaster* embryogenesis (Hinz et al., 1992).
The cis-acting sequences are as follows:
sm1: early expression in the somatic mesoderm and dorsal vessel
sm2: expression in a subset of somatic muscles
sm3: late expression in the somatic mesoderm
vm1: expression in the abdominal region of the visceral mesoderm
vm2: expression in the entire visceral mesoderm

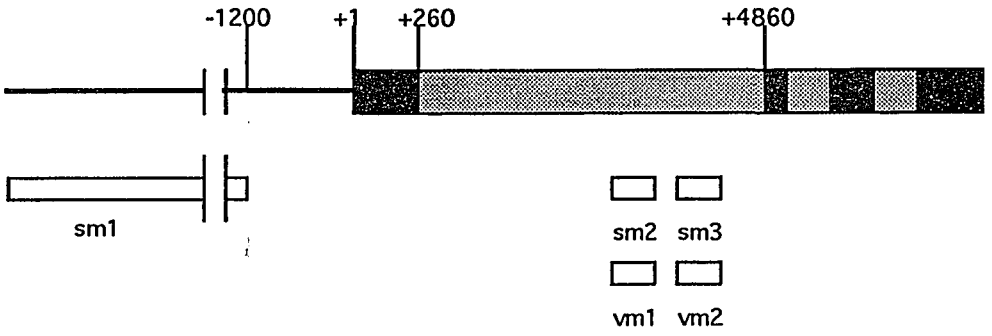

2. MATERIALS AND METHODS

2.1 Bacterial strains

Plasmids for use in microinjections, gel-shift assays and footprinting were propagated in LM1035. This is a derivative of HB101. Uridine containing DNA for mutagenesis was synthesized in CJ236. This E. coli strain is F-dut ung1 thi-1 relA1/pCJ105 (Cm^r)

2.2 Standard procedures

Transformation. Plasmids were made competent via the calcium chloride procedure and transformation was carried out according to standard procedures (Sambrook et al., 1989).

DNA purification. Plasmid DNA was purified by cesium chloride-ethidium bromide density gradient centrifugation (Sambrook et al., 1989).

DNA sequencing. Sequencing was performed by the dideoxynucleotide chain termination method described in the Sequenase version 2.0 Sequencing kit (United States Biochemical, Cleveland, OH).

5' end labelling. Oligonucleotides were labelled with ^{32}P according to standard procedure (Sambrook, 1989). $^{32}P\gamma ATP$ and T4 Polynucleotide Kinase were purchased from New England Nuclear (Boston, MA) and New England Biolabs (Beverly, MA), respectively. Labelled oligonucleotides were purified away from unincorporated $^{32}P\gamma ATP$ on a Cellex D column (Bio-Rad, Hercules, CA). Oligonucleotides to be used for mutagenesis were kinased as above except that unlabelled ATP was used.

Protein Quantitation. Protein concentration was measured by the method of Bradford (1976).

2.3 Mutagenesis with phenotypic selection

In vitro mutagenesis was as described by Kunkel et al. (1987) with some modifications. DNA fragments that contained the regions to be mutated were subcloned in pGEM9zf- (Promega, Madison, WI) and transformed into CJ236. Single stranded uracil-containing DNA was prepared according to standard procedure (Promega Protocols and Applications Guide). Oligonucleotides used for mutagenesis were synthesized by the DNA Core Facility of the Mount Sinai Medical Center). Oligonucleotides used were as follows: 1) SPK1 ($^{5'}$CTGCAAGTGCACGATGTCGACCATGGTGTCTGTA GT$^{3'}$); and 2) SPK10 ($^{5'}$GTCCTACTGAGATCTCCTGTTG$^{3'}$). Second-strand synthesis was carried out using Sequenase Version 2 (United States Biochemicals) and T4 DNA Ligase (New England Biolabs). Mutated plasmids were propagated in LM1035, an ung^{+} strain.

2.4 Polymerase chain reaction

Polymerase chain reaction (PCR) was carried out according to standard procedure (Sambrook et al., 1989) with Vent Polymerase (New England Biolabs). Template DNA came from a single bacterial colony that was lysed at 90° C for 5 minutes prior to PCR. The following is a list of oligonucleotides and their locations (see fig. 3 for sequence):

SPK11	-62 to -42
SPK13	-242 to -220
SPK5	-272 to -254
SPK14	-291 to -266
SPK15	-348 to -327
SPK6	+22 to +4

SPK10	+37 to +16
M13/REV	+366 to +349

2.5 Constructs for functional analysis

The parent plasmid p33B, contains a 2.3 kb *Eco*R I fragment from the genomic oocyte β-tubulin clone λ33, in pGEM9zf- (fig. 2). To construct the non-autoregulatable mutant, pSal33B, p33B was *in vitro* mutagenized with oligonucleotide SPK1 (fig. 4). The mutation was designed such that a *Sal* I site was created at +64, and the amino acid sequence MREI was changed to MVYI.

pSal33BSPK5-EcoRI was constructed by PCR of pSal33B with SPK5 and M13/REV as the 5' and 3' oligonucleotides (fig. 6A). *Eco*R I sites are found in SPK5 and in the 3' polylinker region upstream of the REV binding site. Digestion of the PCR product with *Eco*R I and subcloning into pGEM9zf- produced a deletion mutant that contained 272 bp of regulatory sequence.

p33BHindIII-EcoRI was created by deleting the *Hind* III fragment from p33B. *Hind* III sites are located at -121 and at the 5' polylinker region.

The reporter plasmid used for all promoter deletion analyses by the chloramphenicol acetyltransferase assay, was pBLCAT6 (G. Schutz, German Cancer Research Center, Heidelberg, Germany). This vector contains the chloramphenicol acetyltransferase gene (CAT), the SV40 small t-intron, and the β-lactamase encoding gene. There are three SV40 polyadenylation signals, one downstream of the small t-intron and two upstream of the 5' polylinker (fig. 8).

To release the promoter from p33B, a *Bgl* II site was created at +23 by *in vitro* mutagenesis with SPK10, creating

pBglII33B. Digestion with *Bgl* II and *Xba*I released a fragment encompassing an upstream region that is approximately 600 bp less than the 33B upstream region, and nucleotides to +23. This was subcloned into an appropriately restricted pBLCAT6 vector, creating the clone p33BXbaI-BglII (fig. 9).

Deletion mutants were created by PCR of pBglII33B. Initially, promoter fragments were synthesized using SPK10 at the 3' end and various oligonucleotides that delineated the 5' ends of the mutants. These 5' oligonucleotides were designed such that they had an XbaI site. *Xba*I /*Bgl* II digested PCR fragments were subcloned into pBLCAT6. p33BSau3AI-BglII was generated by first subjecting pBglII33B to PCR with SPK13 and SPK10 as the 5' and 3' oligonucleotides, respectively. The PCR product was digested with *Bgl* II (in SPK10) and *Sau*3A I (at -177). *Sau*3A I and *Bgl* II ends are compatible therefore, the digested fragment was subcloned into a *Bgl* II digested pBLCAT6 vector. p33BHindIII-BglII was constructed by deleting the *Hin*d III fragment from pBglII33B. HindIII sites are at -121 and in the 5' polylinker of pBLCAT6. A summary of the deletion mutants can be found in figure 10.

2.6 Maintenance of *Xenopus laevis*

Adult *Xenopus laevis* were obtained from Xenopus I (Ann Arbor, MI). Frogs were housed in dechlorinated tap water at 18-20° C. Day/night cycle was maintained at 15/9 hours respectively. A more detailed description of *X. laevis* maintenance can be found in Goldin (1992).

2.7 Preparation of oocytes for microinjection

Frogs were anaesthetized prior to surgery by immersion in

iced water. Removal of oocytes and collagenase treatment were performed according to Goldin (1992) with some modifications (Boaz Gillo, pers. comm.). Oocytes were teased in Ca^{+2}-free ND96 (96 mM NaCl, 2 mM KCl, 1 mM $MgCl_2$, 5 mM HEPES-NaOH pH 7.5) and treated with 2 mg/ml Collagenase A (Boehringer Mannheim, Indianapolis, IN). When the majority of oocytes were separated and defolliculated, collagenase was removed by rinsing the oocytes several times in ND96 (Ca-free ND96 + 1.8 mM $CaCl_2$). The largest and undamaged oocytes were incubated in ND96E (ND96 supplemented with 100 µg/ml penicillin, 100 µg/ml streptomycin, 0.5 mM sodium phosphate and 2.5 mM Pyruvate) at 20° C. Oocytes were stored for a maximum of 4 days prior to microinjection.

2.8 Microinjection

Only stage V/VI oocytes (section 1.13) were selected for injection. Twenty nanoliters of CsCl purified plasmid DNA in TE was injected into the germinal vesicle. The device used for microinjection consisted of a 10 µl microdispenser (VWR Scientific, San Francisco, CA) mounted on a three-dimensional coarse manipulator. Delivery into the nucleus was approximated by aligning the needle with the center of the animal pole, perpendicular to the equatorial plane, and displacing 300 microns into the oocyte. Injected oocytes were incubated at 20° C in ND96E.

2.9 RNA Isolation and primer extension

At the end of the 3 hour incubation period, the buffer was removed and oocytes were stored at -80° C. Lysis buffer (20 mM

Tris-HCl pH 7.5, 100 mM NaCl, 1 mM EDTA, 1% SDS) supplemented with 0.2 mg/ml Proteinase K (Boehringer Manheim) was added to the frozen oocytes (Probst et al., 1979). Lysis was achieved by vigorous vortexing after which oocytes were incubated at 37° C for 30 minutes, extracted thrice with phenol/chloroform and once with chloroform:isoamyl alcohol. Samples were brought to 0.3 M sodium acetate, precipitated, resuspended in 10 µl dH_2O per oocyte, and stored at -80° C.

Primer extension analyses were performed using 0.5 oocyte equivalents of RNA and 0.5-0.6 ng (2.5 X 10^5 to 6 X 10^5 cpm) of the appropriate primers. Annealing was carried out in a hybridization buffer containing 0.4 M NaCl, 40 mM PIPES (pH 6.5) and 1 mM EDTA. RNA and primer were heated to 80° C for 3 minutes and incubated for 2 hours at either 55° C (H4 and Xlo primer) or 50° C (SPK9 primer). After precipitation, specific RNA was elongated in 50 mM Tris-HCl (pH 8.3), 75 mM KCl, 3 mM $MgCl_2$, 0.5 mM each dNTPs, 0.2 µg of Actinomycin D, 5 mM DTT, 20 units RNase inhibitor (Promega), and 18-22 units of Murine Moloney Leukemia Virus Reverse Transcriptase (M-MLV RT, Gibco BRL, Gaithersburg, MD) for 1 hour at 42°C. The reaction was stopped by heating at 80°C for 10 minutes. Elongation products were dried, resuspended in sequence loading buffer (98% deionized formamide, 10 mM EDTA pH 8.0, 0.025% xylene cyanol FF, 0.025% bromophenol blue) and electrophoresed through an 8% sequencing gel. Signals were quantitated by phosphorimager analysis (Molecular Dynamics).

2.10 Protein isolation and CAT assay

Microinjected oocytes were incubated for 24 hours, after which ND96 was removed and replaced with 50 µl/oocyte 250 mM

Tris-HCl (pH 8.0). Oocytes were homogenized by pipetting up and down prior to quick-freezing. Oocytes were subjected to two freeze/thaw cycles in dry ice and at 37° C respectively. The oocyte suspension was microcentrifuged at 4° C for 15 minutes and the supernatant was stored at -80° C. Typically, 5 µl of the supernatant (0.1 oocyte equivalent) was used in a standard CAT assay (Gorman, 1982). Thin layer chromatography plates were exposed to a phosphorimager screen for quantitation (Molecular Dynamics).

2.11 Substrates for *in vitro* analysis

The fragment 33BSPK5-SPK6 was synthesized by PCR with pSal33B as the template, and SPK5 and SPK6 as the 5' and 3' oligonucleotides, respectively. These oligonucleotides contain *Eco*R I sites at their termini. The PCR product was digested with *Hin*d III and *Eco*R I, and the 2 fragments generated were subcloned into pGEM9zf-. The resulting constructs, p33BSPK5-HindIII and p33BHindIII-SPK6 contained promoter regions spanning nucleotides -272 to -116 and -121 to +21, respectively (fig. 14).

DNA fragments for gel-shift and footprint analyses were labelled by first linearizing the above constructs with *Hin*d III or *Eco*R I and filling-in with ^{32}PαdCTP or ^{32}PαdATP, respectively. Reactions were carried out in the restriction enzyme buffers supplemented with 0.03 mM each of the three unlabelled dNTPs and 5U Klenow DNA Polymerase I Enzyme (New England Biolabs, Berverly, MA). Following extraction and precipitation, the inserts were released from the vector by digestion with *Eco*R I or *Hin*d III. Labelled fragments were electrophoresed on a 5% native

polyacrylamide gel and the appropriate bands were excised. After electroelution in 0.1X TBE (9 mM Tris pH 8, 9 mM Boric acid, 0.2 mM Na_2EDTA), DNA was extracted, precipitated and resuspended in dH_2O.

Competitor fragments for gel-shifts were generated by first releasing 33BSPK5-HindIII or 33BHindIII-SPK6 with *Hin*d III and *Eco*R I. Fragments were then purified using the Mermaid kit (Bio 101, La Jolla, CA). Non-specific competitors were generated by digestion of pGEM9zf- with *Msp* I and Mermaid purification of the 110 and 149 bp fragments.

pXls11 contains the HindIII fragment of the Xenopus laevis 5S somatic RNA gene (Peterson, 1980) in pBR322. The XlsII fragment for footprinting was prepared as above. Initial restriction and labelling was at the HindIII sites and the fragment of interest was released with *Apa* I. This 329 bp fragment contains 48 bp of the 5' non-coding region, the entire 5S RNA gene and 161 bp of 3' non-coding sequence.

2.12 Preparation and purification of total ovary extract

Crude total ovary extracts from total ovaries were prepared according to Scotto, et al. (1989). DNA binding proteins were purified on a Heparin Sepharose column (Pharmacia LKB Biotechnology, Piscataway, NJ) equilibrated with oocyte lysis buffer (50 mM Tris-HCl pH 8.4, 170 mM KCl, 0.2 mM EDTA, 20% glycerol, 0.5 mM DTT, 0.1 mM PMSF, 10 µg/ml Leupeptin, and 10 mM TAME). The crude extract was microcentrifuged for 15 minutes to remove any insoluble material and the supernatant was directly loaded onto the column. After extensive washing in oocyte lysis buffer to remove non-binding proteins, DNA binding

proteins were eluted in oocyte lysis buffer with 0.4 M KCl. Elution with 1M KCl in the same buffer removed tightly bound proteins. Eluants were quick-frozen and stored at -80° C.

2.13 Isolation of oocyte nuclei

To obtain total nuclear protein, nuclei were manually isolated from oocytes. A small hole was made with a 19 gauge needle at the center of the animal hemisphere. The nucleus was then ejected by squeezing the oocyte with a forcep. Groups of 10 nuclei were collected in ND96 supplemented with 20% glycerol, lysed, and quick-frozen.

2.14 Gel mobility-shift assays

Gel-shift assays were performed according to Garner and Revzin (1981). Total oocyte protein was preincubated for 10 minutes at 0° C with 1.5-7 μg of poly d(I-C) (Pharmacia, Piscataway, NJ) in a buffer composed of 40 mM Tris pH 7.9, 54 mM KCl, 5 mM MgCl, 10% glycerol, and 0.5 mM DTT. Competition experiments were performed by adding 100- to 200-fold molar excess of competitor DNA during the preincubation period. One ng of end-labelled fragment was added and protein binding was carried out at 0° C for 60 minutes. The reaction mixture was electrophoresed through a 5% polyacrylamide gel in 0.5X TBE.

When total nuclear protein was used preincubation was in a buffer containing 64 mM NaCl, 100 mM KCl, 55 mM HEPES-NaOH pH 7.8, 1 mM DTT and 1.5 μg poly d(I-C) for 10 minutes at 0° C. Binding to labelled fragments was carried out at 0° C for 60 minutes. The competitors and fragments used are described in each figure.

When Heparin-Sepharose purified proteins were used,

preincubation of various protein fractions was in a buffer containing 40 mM Tris pH 7.9, 115 mM KCl, 5 mM MgCl, 10% glycerol and 0.5 mM DTT for 10 minutes at 0° C. Poly d(I-C) concentrations are described in each figure.

2.15 DNase protection

DNase I footprinting was performed using a modification of the technique described by Galas and Schmitz (1978). Conditions for protein binding were as for band shift assays. After incubation, samples were brought to 2.5 mM $CaCl_2$ and digested with DNase I (Boehringer Mannheim). When samples were to be electrophoresed directly on a 7% sequencing gel, reactions were terminated by the addition of 120 µl of 12.5 mM EDTA, 10 µg/ml Proteinase K, 125 µg/ml yeast tRNA and 0.1% SDS and incubated at 37° C for 15 minutes. Samples were extracted with phenol/chloroform/isoamyl alcohol, ethanol precipitated, resuspended in sequence loading buffer (90% formamide, 0.1 mM EDTA, 0.1% xylene cyanol and 0.1% bromophenol blue) and electrophoresed. Footprints were judged by comparison to DNase digested naked DNA and sized with G and A/G Maxam-Gilbert sequencing reactions (1980).

2.16 Autoregulatory constructs

Two constructs used to test autoregulation were described in section 2.5 (p33B and pSal33B). p33BEcoRI-HgiAI was constructed by digesting the 33B/*Eco*R I fragment with *Hgi*A I at +72. The fragment containing the upstream sequence and nucleotides to +72 was subcloned into an *Eco*R I/*Nsi* I digested pGEM9zf- vector.

2.17 Purification of erythrocyte and oocyte tubulin

Xenopus laevis erythrocyte cytoskeletons were isolated by the procedure for isolating dogfish marginal bands (Cohen and Ginsburg, 1986). *X. laevis* oocyte-tubulin was purified by the method of Jessus et al. (1985). Protein concentrations were determined by the method of Bradford (1976).

2.18 SDS-polyacrylamide gel electrophoresis

Prior to electrophoresis, erythrocyte and oocyte tubulin samples were adjusted to 50 mM Tris pH 6.8, 100 mM DTT, 2% SDS, 0.1% Bromophenol Blue and 10% Glycerol. Alpha- and beta-tubulin was separated on a 6% sodium dodecyl sulfate-polyacrylamide gel according to the method of Laemmli (1970). Proteins were visualized by silverstaining (National Diagnostics, New Jersey, USA) or transferred to nitrocellulose for western analysis.

2.19 Preparation of antisera against erythroid β-tubulin

Polyclonal antibodies were raised in a New Zealand White rabbit. Erythroid microtubules were prepared by the method described above and the α– and β-tubulin bands were visualized on a preparative SDS-PAGE by Coomasie Blue Staining. The erythroid-specific β-tubulin band was excised, crushed, acetone precipitated and lyophilized. The dried gel was rehydrated with 2 ml phosphate buffered saline and 1 ml Freund's complete adjuvant. After one round of homogenization, the emulsion was successively passed through a 20, 21 and 22 gauge needle, rehomogenized with a tighter pestle, and passed through a 23 gauge needle.

The antigen was injected subdermally on days 1, 15 and 75.

Blood was collected on days 24, 40, 47 and 88. To obtain antisera, the blood was allowed to clot at 37° C for 30 minutes and incubated at 4° C overnight. The serum was filtered through cheesecloth and centrifuged at 1000 g for 5 minutes to remove lysed red blood cells. The supernatant was used directly for Western analysis or aliquoted and stored at -80° C.

2.20 Analysis of antisera

Western analysis was performed according to the method of Burnette (1981). Immunoreactivity of the antisera was tested by first blocking the protein containing nitrocellulose sheets with 1% BSA. The blot was then incubated with a 1:100 dilution of serum in tris buffered saline in tween 20 (10 mM Tris pH 8.0, 150 mM NaCl, 0.5% Tween 20). Alkaline phosphatase-conjugated anti-rabbit IgG was used as the secondary antibody and the antigen antibody complex was detected by coloration with nitro blue tetrazolium and 5-bromo-4-chloro-3-indolyl phosphate (Promega).

3. FUNCTIONAL ANALYSIS OF *Xlot*

3.1 Introduction

Within an organism, microtubules form a multitude of structures with distinct functions. Specification of structure is controlled in part by the ratio of various tubulin isotypes. This is in turn regulated by the selective transcriptional activation of members of the α– and β-tubulin gene families. Transcriptional regulation is based on the interplay between cis-acting elements in the DNA and trans-activating factors available in different cell types.

This thesis addresses β-tubulin gene expression in *Xenopus laevis* oocytes by focusing on the oocyte β-tubulin gene, *Xlot*. This study represents the first analysis of a vertebrate β-tubulin promoter. Oocytes provide an ideal model to analyze this promoter because they are the cellular source from which this gene was isolated, and thus provide a homogenous system in which to test *Xlot* promoter function.

To investigate *Xlot* expression in oocytes, we have isolated and cloned a portion of the *Xlot* genomic region. In this chapter we describe the sequence and identification of cis-acting regions that affect *Xlot* expression in microinjected oocytes.

3.2 Results

3.2.1 Sequence analysis

Previous work in this laboratory showed that a 13 kb genomic clone λ33 hybridizes to the *Xlot* cDNA (Bieker, unpublished results). *Eco*R I digestion of this clone yields six fragments as shown in figure 2A. For analysis of potential 5'

promoter sequences, the 2400 bp *Eco*R I "B" fragment containing the *Xlot* 5' untranslated region was subcloned into pGEM9zf-, producing p33B (fig. 2B). The region from -609 (relative to the transcription start site) to +287 (3' end of the B fragment) was sequenced (fig. 3).

Alignment with the *Xlot* cDNA sequence determined that the 33B fragment contained the entire 116 bp first exon and 171 bp of the first intervening sequence. Primer extension of *Xlot* RNA from oocytes determined that 4 transcription start sites are utilized, all of which were missing from the original *Xlot* cDNA clone (Bieker and Yazdani-Buicky,1992). We have identified these sites and determined that the major start site is a U residue. The start sites utilized in early oogenesis and in stage 40 embryos are shown in bold (fig. 3). The 5' splice donor consensus GTGAGT (+117 to +122) is within the exon/intron border. A perfect TATA box consensus (TATAAA) is at -30 to -25 and a putative CAAT box homology AGCCAAT (Chodosh et al., 1988) is at -87 to -81, similar in location to their corresponding elements in many RNA Polymerase II transcribed genes. Additional CAAT boxes are at -138, -193, -237 and -273. Other potential cis-acting elements also found in the only other sequenced class IVb β-tubulin promoter, hβ2 (Lewis et al., 1985), include binding sites for: AP2 at -65 and -199; Sp1 at -65; Polyoma enhancer binding protein at -53, -229, -199 and -298; SV40 T-antigen at -97 and -202; and a metal responsive element of the metallothionein gene promoter at -67.

3.2.2 Identification of substrates for deletion analysis

The partial sequence of the genomic clone enabled us to

analyze the location of 5' upstream flanking sequences that facilitate transcription. To avoid the possibility of co-translational RNA autoregulation (section 1.9), we first mutated the autoregulatory signal MREI to the non-functional sequence MVYI (Yen et al., 1988b; fig. 4). The nucleotide sequences encoding valine and tyrosine (+63 to +68) correspond to a *Sal* I . restriction site, thus the resulting plasmid was termed pSal33B.

To determine whether microinjected pSal33B was capable of directing transcription in oocytes, primer extension assays were utilized to measure the level of plasmid-encoded RNA. Transcription from pSal33B is initiated at +1 of the tubulin sequence and proceeds through pGEM9zf- sequences. Primer extension using SPK9 (+92 to +63) will not detect endogenous tubulin mRNA as it can hybridize only to RNA that is derived from pSal33B and contains the mutant *Sal* I sequence. Because stage V/VI oocytes utilize only the major start site (section 1.11), the extended product with SPK9 was expected to be 92 bases long. In addition to the test plasmid, a marked histone gene, pH4M:H1 (J. Thompsen, SUNY Stonybrook) was co-injected as an internal control. pH4M:H1 is marked by a *Hind* III linker inserted 160 bp into the coding sequence, and the oligonucleotide JTH4 is designed such that it does not recognize endogenous histone mRNA (J. Thompsen). Primer extension of properly initiated histone generates 181-187 bp products due to multiple start sites of transcription.

To test for pSal33B functional activity, equimolar amounts of pSal33B and pH4M:H1 were coinjected into 6 groups of oocytes in pools of 10. Following a 3 hour incubation in which 95-100% of oocytes survived, total RNA was extracted and plasmid-derived tubulin and histone transcripts were quantitated.

In control experiments with uninjected oocytes or oocytes injected with the pGEM9zf- vector alone, primer extension of up to 2.5 oocyte equivalents with SPK9 did not show an extended product (data not shown). Thus, SPK9 does not recognize endogenous tubulin RNA. The construct of interest, pSal33B is transcribed at an easily detectable level. Each lane in figure 5 represents extension from only half an oocyte equivalent from a pool of 10 oocytes. We observed the appearance of multiple bands surrounding the appropriately sized product, as well as one that is significantly larger. The multiple bands: 1) could represent prematurely terminated primer extension products; or 2) could be due to multiple start site utilization, a phenomenon observed in stage I/II and III/IV oocytes (Bieker and Yazdani-Buicky, 1992).

The significant level of transcription from pSal33B indicated that cis-regulatory sequences are present within the 2000 bp upstream region of the 33B fragment. However, to narrow the scope of our studies, a shorter upstream region that was still capable of driving transcription was identified. To this end, pSal33BSPK5-EcoRI was utilized. It is unlike pSal33B only in that it contains 272 bp of the 2000 bp upstream regulatory region (fig. 6A). Upon microinjection, this deleted construct was capable of driving a significant level of transcription (fig. 6B), as detected by primer extension with the oligonucleotide Xlo (+38 to +18). In addition, it shows the same start site utilization pattern as pSal33B (fig. 6C).

In summary, we have identified two tubulin constructs with 2000 bp and 272 bp of upstream sequence that are capable of facilitating transcription from similar start sites. Since correctly initiated transcription indicates the presence of

appropriate cis-acting regions, these constructs could be used as the starting reagents for deletion analysis.

3.2.3 Identification of the aberrant transcript

We were concerned about the large extension product (seen in fig. 5), as aberrant transcription from microinjected templates is a recurring problem in oocytes, and subsequent deletion analyses were to be carried out using the CAT assay system. Unlike primer extension, the enzyme system does not distinguish between the real and aberrant transcripts, and therefore transcriptional activity can be misrepresented.

Attempts were made to determine whether the large extension product was due to: 1) an artifact of microinjection; 2) RNA synthesized from aberrant transcription initiation; or 3) priming within the RNA 3' to the actual SPK 9 binding site. Injection with the control template pGEM9zf- alone did not result in transcription of a large RNA species from the endogenous gene. Therefore the large primer extended product is not an artifact of injection.

Additional experiments were undertaken to determine if the second or third possibilities explained the appearance of the large product. Initially, size determination of this product was accomplished by co-electrophoresis of primer-extended RNA with an SPK9/pSal33B sequencing reaction. This approximately 310 bp band is 220 bases larger than the expected product. If cryptic transcription initiation at -220 was the cause, a construct with only 123 bp of upstream sequence (pSal33BHindIII-EcoR1; fig. 7A) would not be expected to direct transcription of this larger RNA species. Similar sized extended products were observed from oocytes injected with the full length construct pSal33B (fig. 7B,

lanes 2 and 3) and pSal33BHindIII-EcoR1 (fig. 7B, lane 1). Thus it appeared that SPK9 was binding at a downstream site, and priming with a different oligonucleotide would produce one set of extended products. However, primer extension with the oligonucleotide Xlo (+38 to +18) did not abolish the aberrant product (fig. 25, lanes 1-3) indicating that the large product originated from a large transcript. Taking into account the results in figure 7, it appears that the larger RNA must be initiated 220 bases upstream of +1 regardless of the length of upstream sequence. This aberrant transcript did not pose a significant problem in the analysis of the CAT assays (section 3.2.4, p. 42).

3.2.4 Deletion analysis

In our hands, primer extension has been a valuable technique for qualitative analysis of plasmid-derived transcripts. However it has not been an effective quantitative determinant of RNA levels. As such, we next decided to utilize a chloramphenicol acetyl transferase (CAT) assay. CAT is the most frequently used reporter enzyme and the assay is widely accepted as an indicator of promoter activity. It has the advantage that no endogenous CAT activity is present in eukaryotic cells.

The promoterless vector pBLCAT6 (Boshart et al., 1992, fig. 8) contains the CAT coding sequence followed by the SV-40 small t-intron and a polyadenylation signal. In addition, it has 2 polyadenylation signals located immediately upstream of the 5' polylinker. These signals force termination of transcripts inappropriately transcribed from within vector sequences, a common caveat of other CAT vectors. To subclone the 33B

promoter, a *Bgl* II site was created at +25 of p33B forming pBglII33B (fig. 9A). Digestion with *Bgl* II and *Xba* I, and subcloning into pBLCAT6, produced the "full-length" construct p33BXbaI-BglII (fig. 9B). The upstream flanking sequence of this construct is approximately 600 bases shorter at the 5' end than the upstream region of p33B. Tubulin coding sequences to +26 are retained, but the autoregulatory signal downstream of the *Bgl* II site in pBglII33B is not. Transcription is initiated within tubulin sequences but the initiator methionine is derived from the CAT gene.

Because a 272 bp promoter was earlier shown to promote a significant level of transcription, a CAT construct with as much upstream sequence was used as the starting material for sequential deletions. Certain deletion mutants were constructed by PCR using various 5' oligonucleotides containing an *Xba* I site and the *Bgl* II-containing SPK10 primer at the 3' end. Appropriately digested products were cloned into *Xba* I/*Bgl* II-digested pBLCAT6 vectors. Other mutants were constructed by deletion and subcloning of a PCR product or deletion of a fragment within a clone. Mutants were designed to be truncated by 40-70 bp relative to the upstream mutant (fig. 10).

The ideal concentration of microinjected DNA (0.00072 fmol) was determined by co-injection of p33BXbaI-BglII and pSVLuciferase (Y. Inagaki, Mt. Sinai Medical Center). At this concentration, the signal from pSVLuciferase was not repressed, indicating no limiting competition for the necessary factors. For functional analysis, five sets of oocytes in groups of 10 were injected with each construct. Typically 90-100% of the oocytes survived.

Each lane in figure 11 represents CAT activity derived from half an oocyte equivalent from each group of 10. Background levels from pBLCAT6 are negligible in the *X. laevis* oocyte system. p33BXbaI-BglII was arbitrarily chosen to represent 100% CAT activity. Comparison of expression level directed by p33BSPK15-BglII to p33BXbaI-BglII indicated that sequences upstream of -336 are necessary for maximal activity, as this construct retained only 49% of "full-length" promoter activity. Removal of sequences between -336 and -275 (p33BSPK14-BglII) resulted in a slight decrease in CAT activity to 43%, indicating the probable absence of a regulatory element. Further deletion to -229 (p33BSPK13-BglII) decreased enzyme activity to 19%. Almost no activity (0.4%) was detected in mutants containing only 121 or 51 bases of upstream sequence (p33BHindIII-BglII and p33BSPK11-BglII).

To further delimit the sequences between positions -229 and -121 that are necessary for transcription, p33BSau3AI-BglII (-177) was compared to the full length p33BXbaI-BglII (fig. 11). CAT activity was determined to be approximately 2.5% of maximum when only 177 bp of upstream sequence is used. This was taken to represent the shortest construct from which CAT activity can be detected. Taken together, these results indicate the presence of three or more positive cis-acting elements downstream of -275, in addition to the basal promoter. Figure 12 is a summary of CAT activity.

As described previously (fig. 8), pBLCAT6 contains polyadenylation signals that terminate transcripts aberrantly initiated within vector sequences. If the large product observed by primer extension (section 3.2.3) was due to inappropriate priming by the oligonucleotide probe within the RNA, then the

quantitation in figure 12 holds true. If the large transcript is due to transcription initiation 220 bp from the appropriate start site, then constructs with 55, 121 and 177 bp of upstream region will not be properly quantitated. Assuming that the larger RNA represents 40% of total RNA (average of available data), then the adjusted values are 0.2%, 0.7% and 4% for the constructs with 55, 121 and 177 bp of upstream sequence, respectively. These values do not change our conclusions that the two shortest constructs are incapable of facilitating transcription and that the 177 bp construct delineates the 5' end of the minimal promoter.

3.3. Discussion

These data describe the first functional analysis of a vertebrate β-tubulin gene. We have tested 1400 bp of upstream sequence modulating *Xlot* expression and determined that CAT activity driven by this promoter region is quite strong. For example, the activity derived from this promoter is comparable to enzyme activity driven by pBLCAT2 (Luckow and Schutz, 1987), a CAT construct containing the thymidine kinase promoter (data not shown). The thymidine kinase promoter has been shown to be highly active in *Xenopus* oocytes (McKnight and Gavis, 1980).

We also determined that a 336 bp upstream region was still capable of driving significant levels of CAT activity (49%) when compared to the 1400 bp upstream region. Thus, we felt confident in focusing our attention to this region in the subsequent deletion analysis. Figure 13 summarizes the CAT activities derived from various deletion mutants and potential cis-acting elements. The term "potential elements" is limited to those sequences common to the human and frog class IVb

β-tubulin upstream regions.

Activity from various chimeric tubulin-CAT expression plasmids were quantitated relative to the activity of a construct containing 1400 bp of upstream sequence. It was shown that the region between positions -121 and +1 is incapable of promoting transcription (0.4%). A TATA and CAAT box are found in this region. Their location classifies the promoter as a classical RNA polymerase II-transcribed gene (Mitchell and Tijan, 1989). Since such genes normally utilize both elements, it is likely that these elements are required but not sufficient for minimal *Xlot* promoter activity. Other potential elements in this region which may play a role in basal promoter activity are the binding sites for AP2, SP1, PEBP 1, SV-40 T-antigen and a metal responsive element. Sequences between -177 and +1 are capable of driving CAT activity at 2% the level of the 1400 bp sequence. We believe that the 5' end of the minimal promoter is contained within nucleotide positions -121 and -177. The CAAT site at -138 is the only sequence between -121 and -177 common to both class IVb promoters. The addition of 52 bp of upstream sequence (to -229) results in a 10-fold increase in CAT activity, from 2% to 19%, the largest change in enzyme activity within the 336 bp region. Potential cis-elements in this region include binding sites for CAAT protein, AP2 and PEBP1. CAT activity doubles when sequences from -229 to -275 are present. There are two more CAAT elements in this region, at positions -237 and -273. The addition of another 61 bp results in a modest increase in CAT activity, from 43% to 49%. This finding can be explained in two ways: 1) The region from -274 to -336 is not functionally significant. Neither the PEBP 1 binding site nor the 23/24 bp region of homology between the frog (-325 to -302) and human

(-345 to -322) promoters is of significance; or 2) Cis-acting elements reside within this region. However by deleting the remainder of the upstream region, elements whose function may require the presence of upstream sequences would not be detected. For example, the 23/24 bp homology is "non-functional" based on deletion analysis. However, the homologous sequence is within a similar region in the human promoter and no significant homology to other promoters is detected when the sequence is aligned to sequences within GENBANK. This indicates that the sequence could even be a class IVb-specific element. It is arguable that this region binds a factor that acts cooperatively and only in the presence of a second protein that binds upstream of position -336. Alternatively, it is possible that a positive and negative element are present in this region, both of which are deleted concurrently and are therefore undetected.

Several studies can be undertaken to further characterize the *Xlot* promoter. The most obvious is to define its 5' and 3' boundaries. Genomic sequences upstream and downstream of the 33B fragment are available (fig. 2A) and could be subjected to deletion analysis. Newly identified promoter sequences could be analyzed for regions of functional significance. These regions can then be tested for their ability to function as enhancers, in a distance- and orientation-independent manner or as upstream elements, in a distance-dependent manner. Identification of cis-acting elements can be achieved using internal deletions and linker-scanning mutants. *In vitro* this can be substantiated by protein binding and DNase protection/methylase interference assays.

Analysis can then be extended to determine the ability of

deletion mutants to disrupt normal expression of *Xlot* in somatic tissues during embryogenesis. Such studies would involve microinjection of the mutated construct into oocytes, *in vitro* maturation, fertilization and analysis of RNA/protein expression in embryos. Likewise, fertilized eggs could be microinjected. This would address whether up-regulation of *Xlot* in germ cells versus somatic tissues is due to a simple mechanism such as the presence of a germ-cell specific/abundant activator or a repressor in all other cell types. Conversely, regulation can be by distinct but overlapping signals, such as that observed for the Drosophila β3 tubulin gene (Hinz et al., 1990; section 1.8).

Functional properties of the *Xlot* promoter in somatic tissues can also be investigated using available *Xenopus* cell lines (Smith and Tata, 1991). Deletion mutants used for microinjections can be transfected into these cells. Such studies would obviate the need for microinjection into oocytes/fertilized eggs and dissection of tadpoles. Cell lines provide accessibility to a pure population of cells derived from one tissue.

An observation made during these studies was that plasmid-derived *Xlot* RNA initiated at multiple sites in injected stage V/VI oocytes, while endogenous *Xlot* RNA from uninjected oocytes utilized only one site. We hypothesize that multiple start site utilization is due to the high rate of β-tubulin transcription brought about by the microinjected template, and thus mimicks the situation in stage II/III oocytes. These oocytes are transcriptionally most active and utilize four start sites of transcription. This phenomenon can result from competition for limiting amounts of transcription factor(s). This hypothesis can be tested by microinjecting lower amounts of the tubulin

construct and monitoring the number of start sites.

Figure 2. Construction of p33B.
(A) A schematic of the 13 kb genomic fragment from λ33B. *Eco*R I digestion produces 6 fragments as labelled.
(B) The 2.3 kb *Eco*R I "B" fragment was subcloned into pGEM9zf-, producing p33B. Approximately 2000 bp of upstream sequence are denoted by a stippled box, transcribed 33B sequence by a filled box and vector sequence by a checkered box. The 3' end-point (+282/EcoRI) was determined by sequencing.

A. lambda-33 genomic fragment

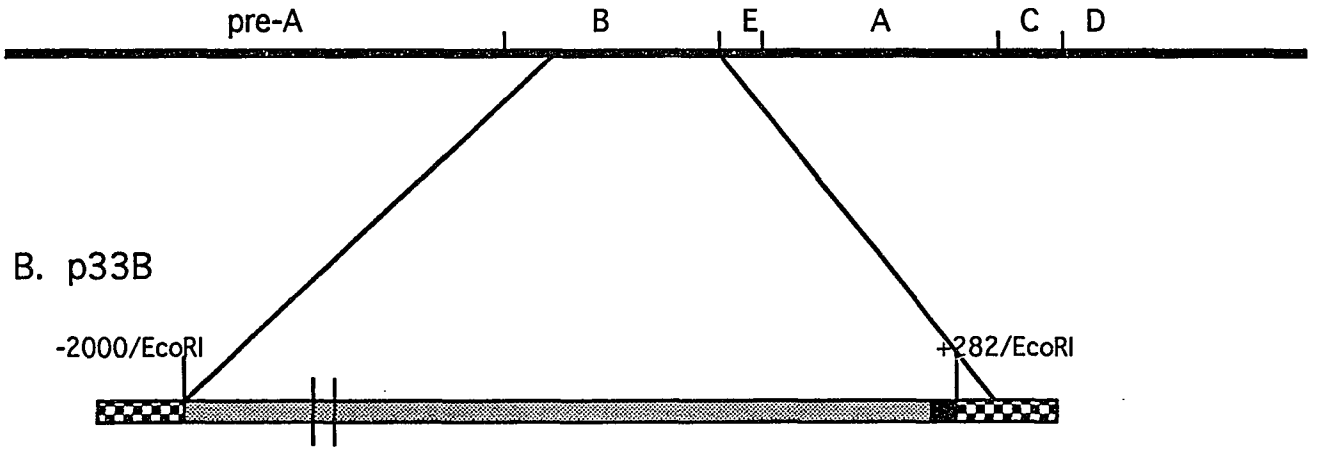

Figure 3. Partial sequence of the 33B genomic fragment.
The region from -609 to +287 of p33B was sequenced. The major start site of transcription is at +1 while minor start sites are at -1, -3 and -4 (boldly ictalicized). The TATA box at -30 is doubly underlined and putative CAAT boxes at -87, -138, -193, -237 and -273 are underlined. The initiator methionine at +60 is boldly underlined. The splice donor site at +117 is overlined.

-609 GAGCGCACGGCACTTTCTGTGAGAAACCATAGCCACAGCGTATGTTTGGGACCC
-555 GTTTCTATACCCATTCCCTCGCCTTGTTGCACACACTAAGGAACTTGTCTGAAC
-501 AAAACGTTGTATCCAGGATAAACACAAATAGGGAGCGGGAACCCACACAGGAT
-448 ATCCCACCAAGCACCATGGCAACCGCAAGTAGCGTAGTCCGGCCCTGACAGCAT
-395 GTGTACGCAAGAGAGAACGCACTTAGTGTTAGGAATAACAATTCGACCGTAGG
-341 TCTTAACGTTTAAGGCGCACTGCGGCGGTTACTAGGACGCCTCTTGCACCACAC
-287 ACTCGTGTTAGGACAGCCAATCACAGTCCTCGTCAATCATTTGAATACGACCA
-234 ATAACAGAGGCTATGTGGACAGTTAGCAGCCCCTCTCCCCCAGCCAATCGTTAT
-180 TAAGATCAGCCCTGTCGGTTTGTATTGACGGACATTCTCCCGACCAATCACAAA
-126 TAGAAAAGCTTGACAACGCTTTGCCGCCTACTTAACTACAGCCAATGGGAAGG
-73 CGAGGGCGGCGCTTGCCCTCTTGAGTCGGCCGTCAGAGCTTCCTATAAAAAGTG
-19 AAGCGCGAGGCAGAC***GT***A***GT***CAGGCGTTTCAAGGCAACAGGAGAGATCAGTAG
+35 GACAGAGCAGTTTACTACAGACACCATGGTCGACATCGTGCACTTGCAGGCTGG
+89 ACAGTGCGGCAATCAGATTGGTGCCAAGGTGAGTTCTATGGGGAGGACGATTAG
+143 ATTTTTTTTTCTCCTCACAGGAGTGGATTGGGGTGGGGCGCAGGTGCCGTGGCTG
+198 GGCCCTAAATCTGCCGTGGCTGGGCCTTAAATCTGCGCTGCCGAGACCATCGCT
+252 TTCCTTTGTGCCTTTGTAGTTCTTTTAATGGGAATTC

Figure 4. Construction of the autoregulatory mutant pSal33B.
Single stranded DNA was synthesized from p33B using the phage f1 origin of replication (filled arrow). Mutagenesis was carried out using SPK1 (mutant oligo) to prime second strand synthesis. The resulting plasmid is pSal33B. The first four amino acids encoded for are Met-Val-Tyr-Ile instead of Met-Arg-Glu-Ile. The sequence GTCGAC is a *Sal* I restriction site. pGEM9zf- sequences (checkered boxes), 33B upstream sequences (stippled box), 33B coding sequence (open box).

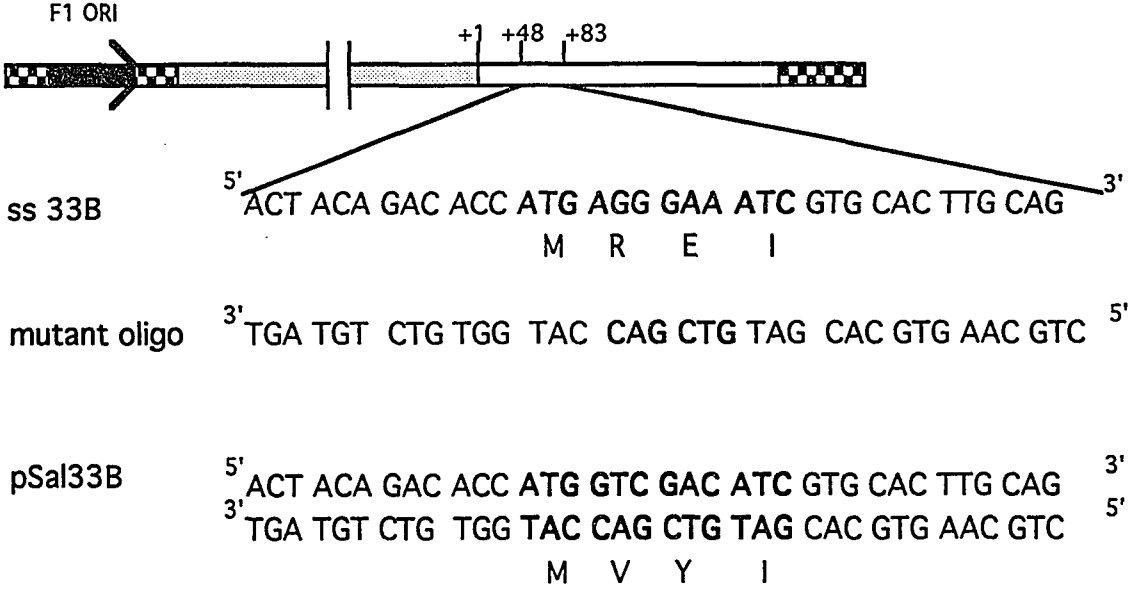

Figure 5. pSal33B-derived transcription in *X. laevis* oocytes. Results of a typical primer extension analysis of total RNA derived from oocytes microinjected with pSal33B. ^{32}P-labelled SPK9 oligonucleotide was used as the primer. A series of bands surrounding the expected 92 bp product is observed (brackets), as is a much larger product (arrow). Each lane represents half an oocyte-equivalent from a pool of 10 oocytes.

Figure 6. Transcription from a 272 bp promoter. pSal33B contains a 2000 bp promoter region while p33BSPK5-EcoRI contains only 272 bp of upstream sequence (A). Primer extension analysis of total RNA from oocytes microinjected with pSal33B (B) or p33BSPK5-EcoRI (C) was compared. Each lane represents primer extension of half an oocyte-equivalent from a pool of 10. Only the bands surrounding the appropriately sized product are shown.

A. Schematic

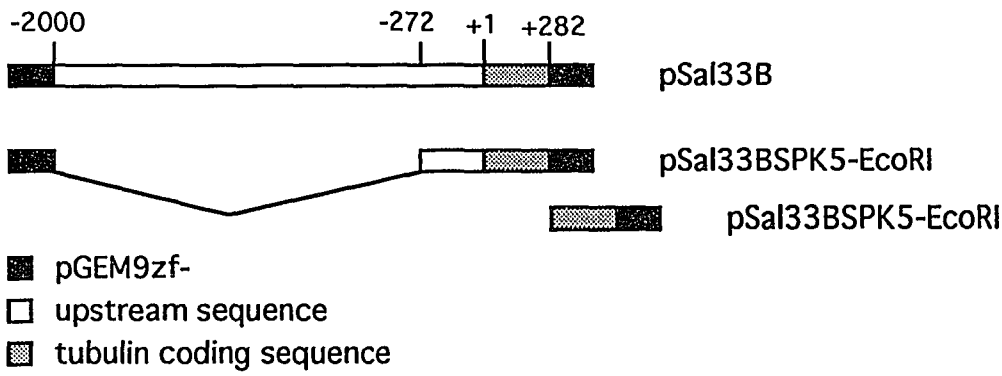

B. pSal33B

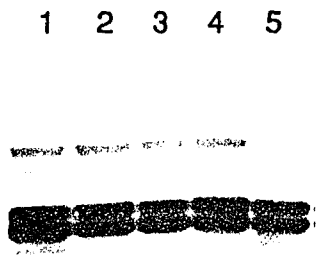

C. p33BSPK5-EcoRI

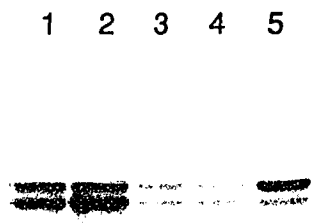

Figure 7. Sizing of tubulin RNA derived from microinjected templates.
(A) pSal33BHindIII-EcoRI which contains only 123 bp of upstream sequence was constructed by deleting a *Hind* III fragment from pSal33B.
(B) Total RNA from oocytes microinjected with pSal33BHindIII-EcoRI (lane 1) or pSal33B (lanes 2 and 3) were primer-extended with SPK9. Each lane represents half an oocyte-equivalent from a pool of 10 oocytes. Similar sized extension products are observed from both sets of RNA. The products surrounding and including the 92 bp product are bracketed. The larger extension product is indicated by an arrow. This product is approximately 220 bp longer than the expected 92 bp product (data not shown).

A. Construction of pSal33BHindIII-EcoRI

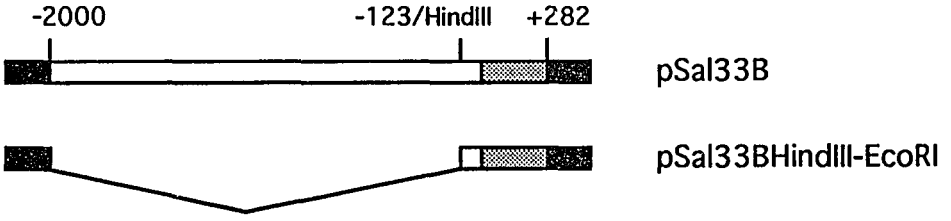

B. Primer extension with SPK9

Figure 8. Map of pBLCAT6.
pBLCAT6 is a 4.25 kb plasmid. It contains three SV40 polyadenylation signals (black boxes), the chloramphenicol acetyl transferase gene (checkered box), the SV40 small t-intron (stippled box) and the β-lactamase encoding gene (hatched box). The polyadenylation signals are divided in two regions. The first is 5' to the cat gene and the second is 3' to the SV40 small t-intron (Boshart et al., 1992)

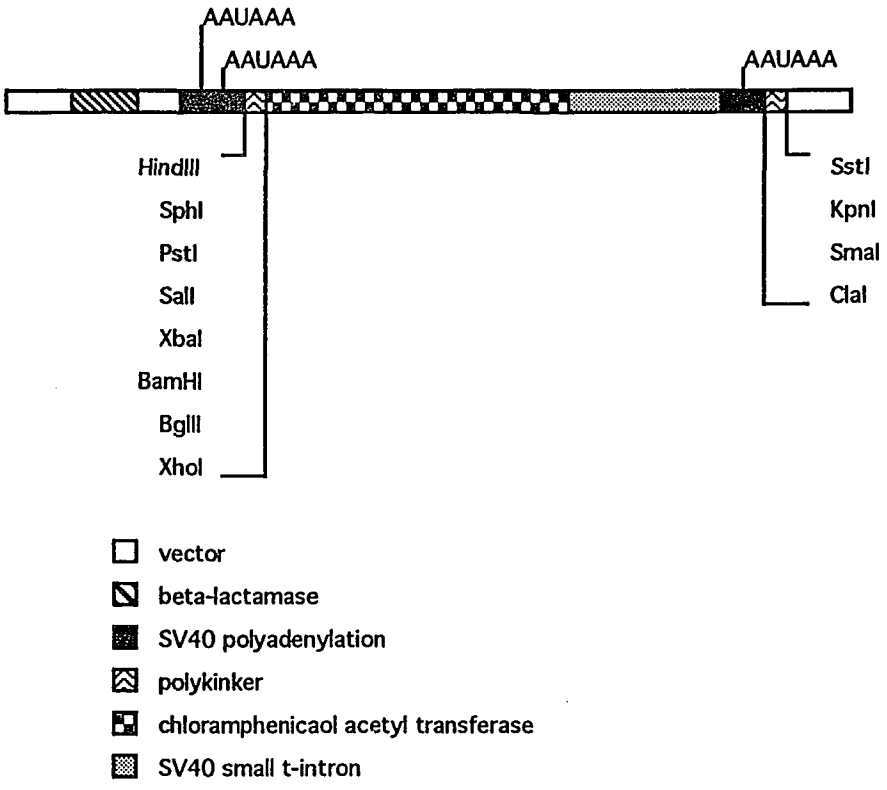

Figure 9. Construction of the "full length" tubulin-CAT fusion, p33BXbaI-BglII.
(A) A BglII site was created at +23 of p33B, producing pBglII33B. *Xba* I sites are located in the 5' polylinker region of pBglII33B and approximately 600 bp from the 5' end of the 33B fragment.(B) pBglII33B was digested with *Bgl* II and *Xba* I, and the 1.4 kb fragment was directionally cloned in pBLCAT6, creating p33BXbaI-BglII. Transcription (arrow) and translation (bold arrow) are initiated within tubulin and CAT sequences, respectively. The co-translational autoregulatory signal of tubulin is downstream of the *Bgl* II site, therefore it is not in p33BXbaIBglII.

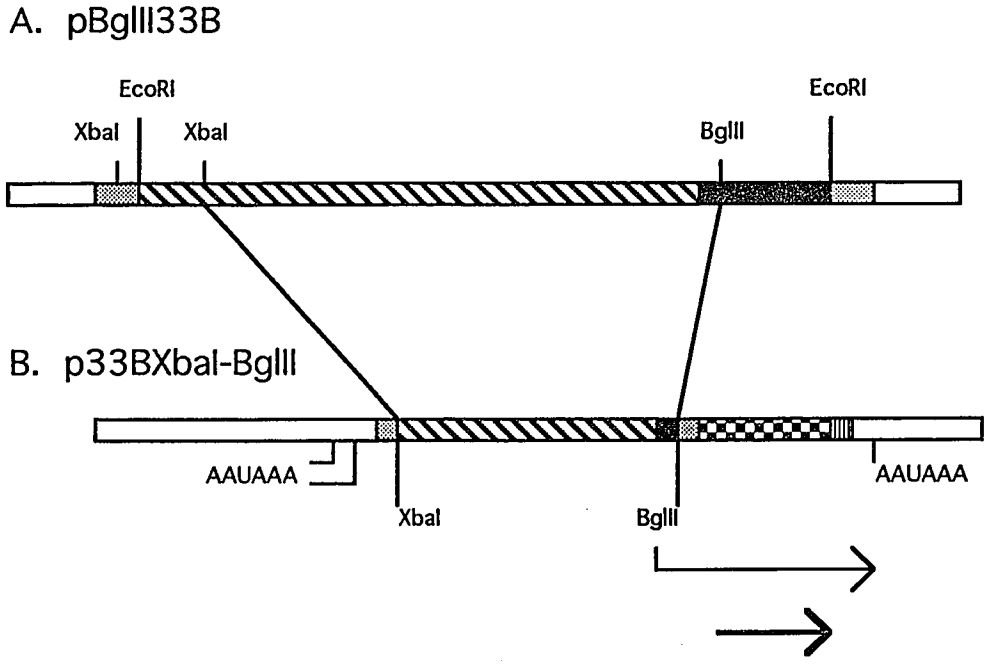

- polylinker of pGEM9zf- in A, pBLCAT6 in B
- 33B upstream sequence
- transcribed 33B sequence
- cat sequence
- SV40 small t-intron
- vector sequence of pGEM9zf- in A, pBLCAT6 in B

Figure 10. Construction of promoter deletion mutants.
Deletion mutants were designed to be truncated by 40-70 bp relative to the upstream mutant. p33BXbaI-BglII is considered the full-length construct. The tubulin-CAT deletion mutants and their 5' end-points are as follows:

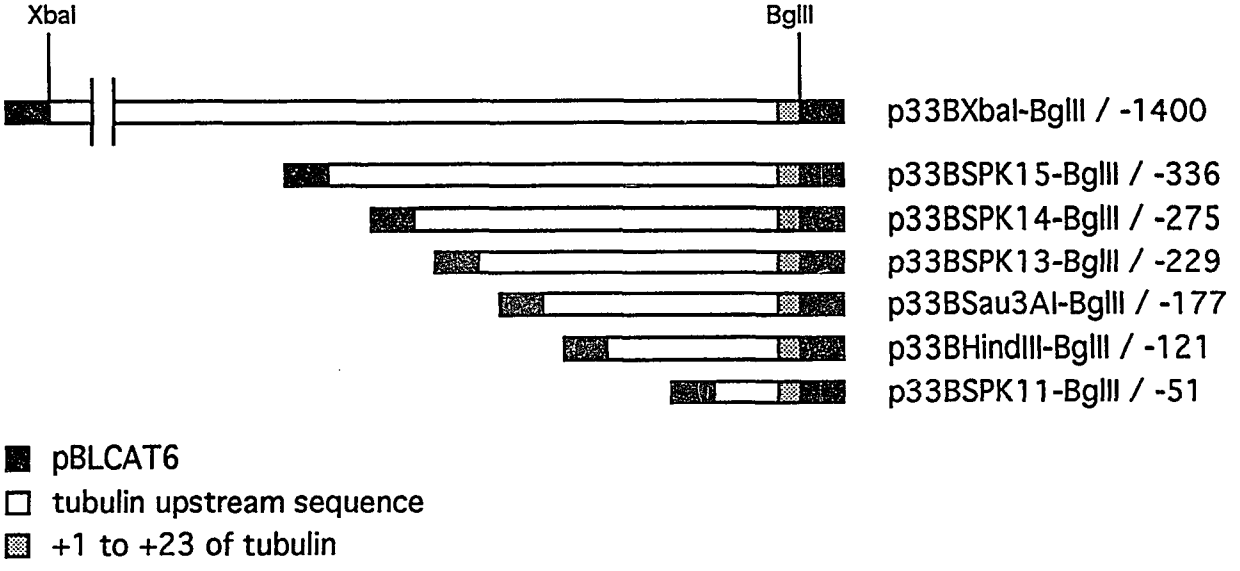

Figure 11. CAT activity derived from tubulin-CAT fusion constructs microinjected into oocytes.
The ability of deletion mutants (fig. 10) to promote transcription was determined. 5 groups of 10 oocytes were injected with each construct and 0.1 oocyte protein equivalents were assayed for CAT acitivity. Each panel is labelled by construct name / 5' endpoint. p33BSau3AI-BglII was assayed separately. Full length and background controls are not shown.

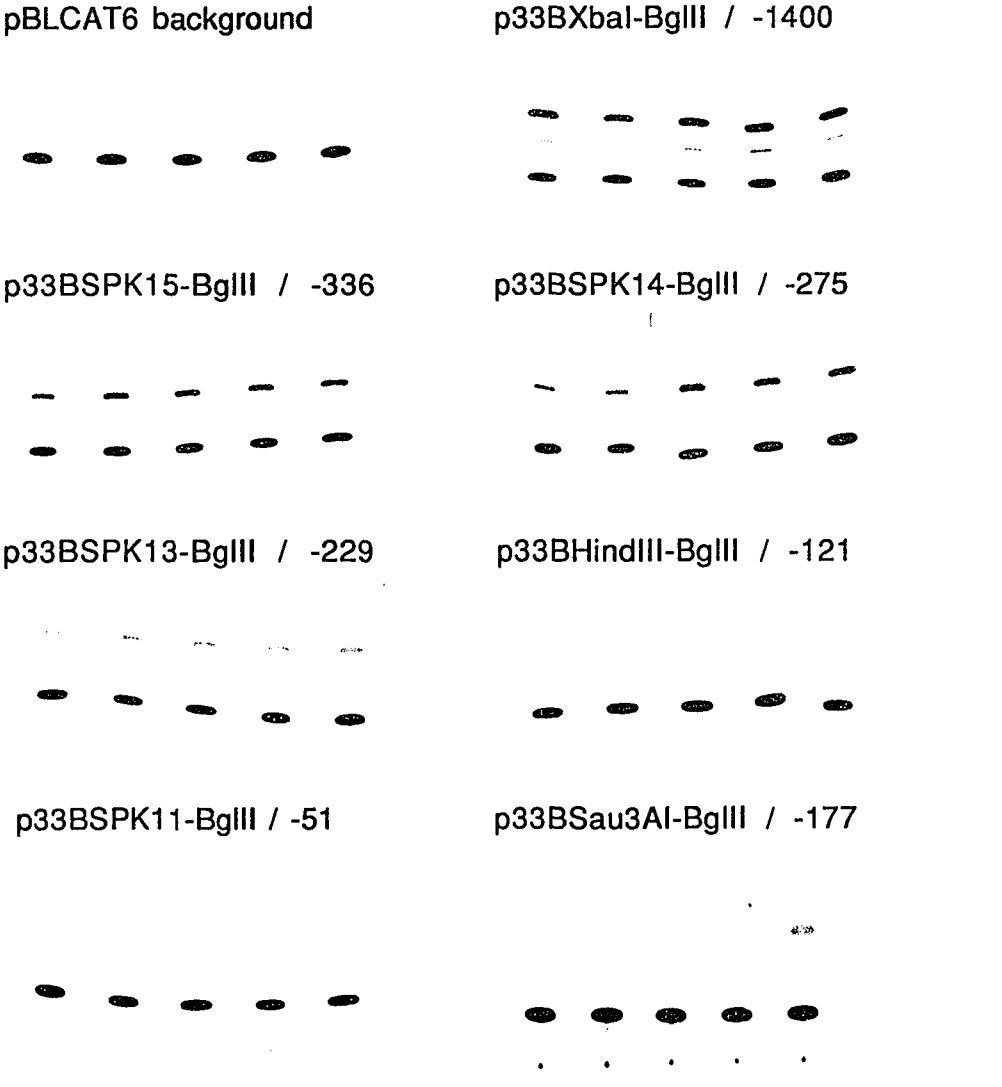

Figure 12. Quantitation of CAT activity from chimeric tubulin-CAT deletion constructs.
Values are expressed as the ratio between CAT activities (+/- S.E.M.) derived from various deletion constructs and p33BXbal-BglII, the full length promoter construct. Each point represents an average of the 5 groups in figure 11.

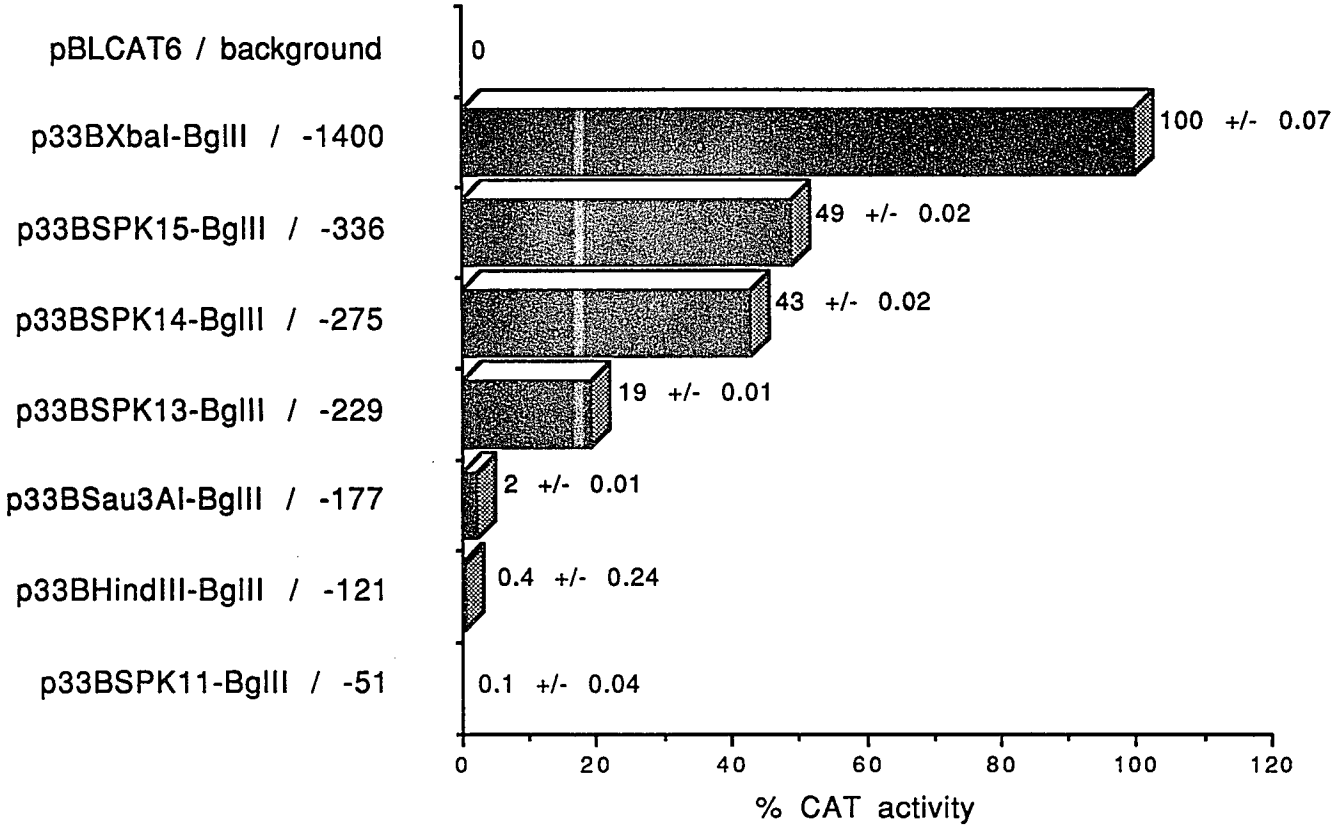
pBLCAT6 / background
p33BXbaI-BglII / -1400
p33BSPK15-BglII / -336
p33BSPK14-BglII / -275
p33BSPK13-BglII / -229
p33BSau3AI-BglII / -177
p33BHindIII-BglII / -121
p33BSPK11-BglII / -51
0
100 +/- 0.07
49 +/- 0.02
43 +/- 0.02
19 +/- 0.01
2 +/- 0.01
0.4 +/- 0.24
0.1 +/- 0.04
0
20
40
60
80
100
120
% CAT activity

Figure 13. Summary of regulatory regions and potential cis-acting elements. A schematic diagram of the tubulin upstream sequence from -336 to +1. The 5' ends of the mutants are indicated below the horizontal line. Vertical lines represent % CAT activity relative to activity from the full-length construct. Abbreviations for potential elements found in both the frog and human promoters, although not necessarily in the same position, are as follows: TATA (TATA box), CAAT (CAAT protein binding site), AP2 (AP2 binding site), SP1 (SP1 binding site), PEBP 1 (Polyoma enhancer binding protein 1 binding site), SV40 TAg (SV40 large T antigen binding site), MRE (metal responsive element from the rat metallothionein gene), 23/24 (23 /24 bp region of homology).

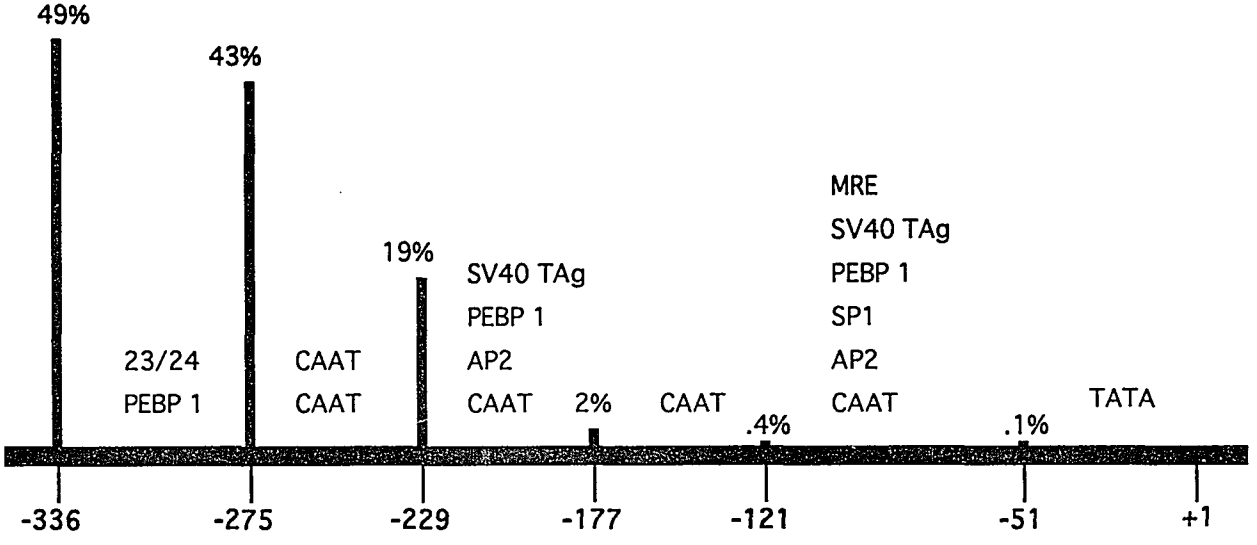

4. IN VITRO ANALYSIS OF TRANS-ACTIVATING FACTORS

4.1 Introduction

In the previous chapter, we identified at least four promoter regions controlling *Xlot* expression in *X. laevis* oocytes. Identification of specific cis-elements responsible for transcription within these regions can be accomplished in several ways. Linker-scanning mutagenesis, which alters a handful of bases without changing DNA topology, represents the most precise method of identifying cis-elements. The use of internal deletions has also been a commonly utilized method. We have taken a biochemical approach to identify these DNA sequences within the 272 bp promoter region directly upstream of the transcription start site. This region is responsible for over 40% of activity relative to a 1400 bp promoter region.

In this chapter we describe gel-retardation and DNase I protection assays aimed at identifying such sequences as well as their cognate binding proteins. The 272 bp upstream sequence was divided into the proximal and distal fragments, the substrates for all protein binding studies.

4.2 Results

4.2.1 Construction of the proximal and distal fragments

We began our studies by synthesizing a PCR fragment using p33B as the template, and SPK5 (-272 to -254) and SPK6 (+4 to +22) as the 5' and 3' primers respectively. The product was digested with *Hind* III (at -121) and *Eco*R I (within the primers), and the two fragments generated were subcloned in pGEM9zf-. These fragments representing the substrates for *in*

vitro analysis were termed: 1) proximal fragment/-121 to +22 and 2) distal fragment/-272 to -116 (fig. 14). The proximal fragment most likely contains most of the sequences responsible for basal promoter activity such as the TATA and CAAT boxes. The distal fragment encompasses 2 identified cis-acting regions responsible for approximately 40% of activity compared to a 1400 bp promoter region. It also contains the 5'-most sequences responsible for minimal promoter activity.

4.2.2 Gel-mobility shift assays with total ovary extract

To screen for oocyte proteins that interact with the 272 bp upstream sequence, a crude cellular extract containing soluble, non-yolk protein, was prepared from a *Xenopus* ovary that contained oocytes representing all six stages of development. This was used in gel-retardation assays with either of the two fragments.

When the proximal fragment was incubated with 16.5 µg of ovary extract and electrophoresed on a native acrylamide gel, two retarded complexes, P1 and P2, could be identified (fig. 15A). The intensity of P2 was consistently less than P1. To test the specificity of these associations, unlabelled homologous and unrelated sequences were used as competitors at a 200-fold molar excess. Competition with the specific, proximal fragment drastically reduced the signal for P1 and P2 (fig. 15A, lane p). The non-specific competitors were the 110 bp (fragment x) and 149 bp (fragment y) fragments from a pGEM9zf-/*Msp* I digest. These fragments were unable to compete for either complex (fig. 15A, lanes x and y). The apparent competition of x for P2 in the figure was not reproducible.

Gel retardation assay using the distal fragment and 33 µg of

crude oocyte extract revealed two complexes, D1 and D2 with similar Rf values to P1 and P2 respectively (fig. 15B). Complex D1 was also consistently more prominent than D2. Specificity of both complexes was demonstrated by the strong competition of 100-fold molar excess of unlabelled distal fragment (fig. 15B, lane d) and lack of competition by both y and x fragments (fig. 15B, lanes y and x).

4.2.3 Comparison of the fragments' binding activities

The similarity of Rf values of the P1/D1 and P2/D2 complexes indicated that similar sized if not identical proteins were binding to both proximal and distal fragments. The ability of the proximal fragment to function as a competitor for D1 and D2 complex formation was next tested.

At a 200-fold molar excess the proximal fragment (fig. 16, lane 4) was as good a competitor for both complexes as the distal fragment (fig. 16, lane 3), when the distal fragment is used as a probe. Both non-specific competitors were unable to compete for the formation of either complex (fig. 16, lanes 5 and 6). The appearance of faster migrating bands in lanes 3 and 4 is an artefact generally encountered in competition reactions. Thus, it appears that binding sites recognized by similar proteins are present in both fragments.

4.2.4 Analysis of potential cis-acting elements

A comparison of the proximal and distal fragment DNA sequences identified binding sites for some trans-activating factors common to both fragments. A single AP2 site is present in each fragment. The proximal fragment has one each of the

CAAT and Polyoma enhancer binding protein 1 (PEBP 1) elements. The distal fragment contains three and two potential binding sites for the CAAT and PEBP 1 proteins, respectively.

CAAT binding proteins are categorized on the basis of their affinity to different DNA binding sites (Chodosh et al., 1988). Of the known CAAT binding sites, that from the adenovirus origin of replication (called NF1; Rosenfeld et al., 1987) is most homologous to the sequence found in the proximal fragment. Since there is only one binding site in this fragment, it was assumed that the CAAT protein must bind here if it is responsible for either complex. The corresponding NF1 oligonucleotide (TTTTGGCTGAAGCCAATATGAG) was unable to compete for binding activity to the distal fragment at a 240- or 480-fold molar excess (fig. 17, lanes 4 and 6; section 4.3, p. 71).

An AP2 and CAAT consensus sequence overlap each other at positions -199 to -187, within the distal fragment. To determine if at least one factor bound within this region, competition experiments were carried out with the corresponding double stranded oligomer SPK7:SPK8 (-203 to -184). This oligonucleotide was unable to compete with the distal fragment for the formation of either complex at a 240- or 480-fold molar excess (fig. 17, lanes 5 and 7). This is in accordance with the lack of NF1 competition and further indicates that the transactivator AP2 does not bind to the distal fragment (section 4.3, p. 71).

4.2.5 Binding properties of the D1 and D2 complexes

Since the two potential cis-elements did not appear to bind their cognate factors, protection from DNase I activity became

the method of choice for identifying possible novel binding sites. The distal fragment was chosen for further analysis because the D1 and D2 complexes appeared to form tight associations. Neither KCl concentrations up to 128 mM nor the absence of magnesium in the binding reaction decreased complex formation (data not shown). In the following kinetic experiment, the proteins were shown to bind for at least 5 minutes. Labelled distal fragment and protein extract were pre-incubated prior to the addition of a 200-fold molar excess of unlabelled specific competitor. Aliquots were taken at one minute intervals and electrophoresed on a non-denaturing acrylamide gel. The intensity of the D1 and D2 complexes did not decrease throughout the 5 minute time period (fig. 18, lanes 0-5) and was similar to that from a competition reaction using fragment x as competitor. This indicated that DNase treatment for up to 5 minutes was possible without the danger of the bound protein coming off the DNA.

4.2.6 DNase I footprint analysis of the distal fragment

The double stranded distal fragment was labeled on the coding strand using the Klenow fragment of polymerase I. The digestion pattern obtained after DNase I digestion of the fragment complexed with total ovary extract, was similar to that from digested, free DNA (data not shown). This background pattern was most likely due to masking by the unbound probe. In the gel-shift experiment above (fig. 15B), only a small fraction (approximately 10%) of the labelled fragment was shifted. The remaining unbound fragment, which was an equal candidate for DNase digestion, could have "covered" any footprinted regions. This problem could be alleviated by complexing all of the labelled

fragment.

4.2.7 Binding activity of an oocyte nuclear extract

On a molar basis the amount of extract would have to be increased 10-fold or labelled fragment would have to be decreased 10-fold to complex all of the labelled fragment. Attempts to shift all labelled fragment by decreasing the amount of DNA and increasing the amount of total ovary extract were unsuccessful. We next reasoned that a protein extract enriched for the binding activity would facilitate complex formation such that all labelled fragment would be shifted. To this end, a nuclear extract was prepared from stage V/VI oocytes. Binding activity of the nuclear extract was compared to that from the total ovary extract in a gel-mobility shift assay with the distal fragment. The ovary extract at concentrations of 30-120 μg facilitated the formation of complexes D1 and D2 (fig. 19, lanes 3-6); however, the signals derived from such complexes decreased with increasing amounts of protein (fig. 19, lanes 4-6). This was most likely caused by the formation of a large non-specific DNA-protein conglomerate that was retained in the wells. With this ovary extract, there is a limit of 30-60 μg, above which the proteins interfere with electrophoresis. Complex formation with 2.5 μg of nuclear extract was two-fold over that found with 30 μg of total ovary extract (new); a 24-fold enrichment in binding activity (fig. 19, compare lanes 3 and 7). In addition, increasing the protein concentration to 10 μg (fig. 19, lane 10) resulted in minimal trapping of the distal fragment in the well.

4.2.8 Footprint analysis with nuclear extract

Conditions that shifted all of the labelled distal fragment using the nuclear extract were not readily obtainable, therefore "footprinting" was carried out on purified, complexed DNA. Adding the purification step facilitates analysis of complexed DNA only. Labelled probe was incubated with 10 µg of nuclear extract and digested with DNAse I. DNA-protein complexes were separated by polyacrylamide gel electrophoresis and detected by autoradiography (fig. 20A). Complexes D1, D2 and the free probe were extracted from gel slices and analyzed on a 7% sequencing gel (fig. 20B). Despite this precaution, we were unable to detect a footprinted region. The digestion patterns obtained from complexed DNA (D1 and D2) were similar to that from unbound fragment.

4.2.9 Properties of heparin-sepharose purified proteins

While a nuclear extract is devoid of cytoplasmic proteins, further enrichment of DNA binding activity can be obtained by heparin-sepharose column chromatography. DNA-binding proteins from a total ovary extract were prepared and protein fractions that were eluted at 0.4 M KCl were analyzed for binding activity. Only complex D1 was detected when the distal fragment was incubated with 13.5 µg of unpurified total ovary extract (fig. 21A and B, lane o). No associations were formed from the wash fraction which should not contain DNA binding proteins (fig. 21A and B, lane w). By definition, DNA binding proteins that bound to the column will bind to any DNA, such as poly d(I-C), non-specifically. Thus, initial binding reactions using the distal fragment and heparin-sepharose purified proteins were devoid of poly d(I-C). Fractions 7 and 8 (fig. 21A, lanes 7 and 8) promoted

retardation of the labelled fragment (D3); however, the complex did not correspond to the D1 complex and was not further characterized. The labelled fragment was retained in the wells when incubated with various 0.4M KCl fractions (fig. 21A, lanes 9-13). This phenomenon could again be attributed to the non-specific DNA-protein conglomerate. To inhibit non-specific protein binding, the purified extract was pre-incubated with 7 µg poly d(I-C) prior to addition of the labelled distal fragment. Under these conditions, complex D3 (fig. 21B, lanes 7 and 8) was abolished while D1 was still detected (fig. 21B, lanes 9-12). The weak signal derived from D1 is attributed to the stringency of the reaction and is further proof for the specificity and strength of this DNA-protein association.

To maximize specific binding and minimize non-specific interactions, poly d(I-C) concentrations were titrated in binding reactions. Increasing the concentration of poly d(I-C) above 0.5 µg (fig. 22, lanes .5-1.5) severely decreased the formation of complex D1. The faster migrating bands (fig. 22, lanes .5 and 1) did not correspond to the D3 complex. Because 0.5 µg poly d(I-C) did not necessarily allow maximal binding of the factor, this non-specific competitor was eliminated from subsequent DNase protection assays. Unfortunately, a footprinted region still could not be detected when the distal fragment was incubated with purified DNA binding proteins (fraction 11 = figure 21B, lane 11), DNase treated and gel purified (data not shown).

4.2.10 DNase footprint analysis of pXIs11

Inability to footprint even the D1 complex was not due to the extracts nor the assay conditions. The 5S somatic RNA gene

pXls11 (Peterson et al., 1980) shows a clear footprint (fig. 23) when incubated with 24 μg of unpurified total ovary extract and digested with DNase I. Our results agree with the known region for transcription factor TFIIIA binding within the coding sequence at nucleotide positions +45 to +96 (Engelke et al., 1980).

4.3 Discussion

We have initiated studies aimed at identifying sequence-specific DNA binding proteins present in *X. laevis* oocyte extracts that interact with the promoter of the germ-cell β-tubulin variant, *Xlot*. Four DNA-protein complexes, two each in the proximal (P1 and P2) and distal (D1 and D2) fragments have been identified (fig. 24). The protein(s) responsible for complexes P1 and P2 are similar to that forming D1 and D2. Three explanations can account for the binding characteristics observed. Within each fragment: 1) Two distinct proteins form either complex, with one more abundant or more tightly bound than the second; 2) One protein recognizes two binding sites with different affinities, with the slower migrating complex resulting from DNA-protein associations at both sites simultaneously; or 3) One protein recognizes a single element, with formation of the larger complex being due to the association of an accessory factor to the smaller, faster migrating, DNA-protein complex.

With the exception of CAAT and the PEBP 1 binding site in the distal fragment, no two known cis-acting elements or short homologous stretches of DNA are present within each fragment. This finding favors the first hypothesis. However, the second hypothesis is still possible if one protein recognizes a second site with partial homology to the true binding site. If such is the

case, the protein is expected to have a lower affinity to this site. Kinetic experiments demonstrated that the signal for the slower migrating complex did not decrease within 5 minutes after addition of excess competitor, an indication of high affinity. The difference between the expected and observed binding properties could be reconciled by the explanation that affinity to the second site is enhanced by the cooperative binding of the proteins responsible for D1 and D2.

Heparin-sepharose chromatography generally enriches for DNA-binding proteins without any attached accessory proteins. When purified ovary extracts were incubated with the distal fragment, both complexes were formed. Unless this is one of the rare cases where accessory proteins remain tightly bound to transactivating factors during purification, D1 and D2 must result from the binding of two distinct DNA binding proteins. Thus, the third hypothesis is unlikely.

The complex D3 can be explained in a number of ways. This association can be due to the binding of a non-specific DNA-binding protein. The activity is present at the front edge of the 0.4M KCl peak, indicating low affinity, and the complex is abolished by incubation with high poly d(I-C) concentrations, indicating a lack of specificity. On the other hand, the protein forming D3 may be the protein responsible for D2, in the 2 element hypothesis. This protein would be a weakly binding protein whose affinity is increased by binding of the protein responsible for D1.

To identify the two binding sites common to both fragments, the proximal and distal fragments' nucleotide sequences were compared. Four known cis-acting elements but no other homologous, potential binding sites were identified. The CAAT

binding site appeared to be the best candidate for a number of reasons: 1) There are four such consensus sequences between positions -81 to -133, while the expected probability of finding a non-random 5 bp motif is approximately 1/1024 bases; 2) The human class IVb tubulin also contains four CAAT sequences; and 3) CAAT binding sites are found in numerous promoters and their binding proteins are ubiquitous trans-activating factors.

The lack of competition by the CAAT-containing NF1 and SPK7:SPK8 oligonucleotides for complex formation with the distal fragment indicated that the corresponding binding protein did not account for this complex. However, this potential association requires further characterization since there are several CAAT proteins whose binding depends not only on the CAAT consensus but flanking sequences as well (Chodosh et al., 1988). It is possible that the CAAT protein binds to the distal fragment but not to NF1 and SPK7:SPK8, by virtue of the sequences surrounding the consensus element. In addition, the CAAT sequence has been postulated to be necessary for the activity of several promoters in oocytes (Scotto et al., 1989; Mc Knight et al., 1981; Middleton, 1989). CAAT-like proteins have also been detected in early blastula embryos. Proteins present before midblastula transition are maternally expressed and are most likely present in oocytes (Ovsenek et al., 1990).

The lack of AP2 binding is indicated by the inability of SPK7:SPK8 to compete with the distal fragment for complex formation. This supports the finding that XAP-2, the *Xenopus* homologue of the human AP2 cDNA, is not expressed in oocytes (Winning et al., 1991). However, it is possible that an AP2-like protein is present within oocytes and its binding requires

additional sequences or a particular DNA topology not present in SPK7:SPK8.

DNase I footprint analysis was carried out in an effort to identify the precise binding sites involved in complexes D1 and D2. Our inability to detect footprinted regions even when the complexed, DNase-treated fragment was isolated is rather perplexing. Theoretically this fraction should only contain purified protected fragment since the complex does not dissociate within the time required for DNase digestion. This result could not be attributed to a binding site at the end of the distal fragment since footprint analysis using fragment labelled on the non-coding strand did not reveal a protected region either (data not shown).

Several studies can be carried out to define the nature of the tubulin promoter-oocyte protein complexes: 1) The binding sites for the CAAT, AP2, SV-40 TAg, and PEBP 1 proteins represent 12 potential binding sites. Each site can be tested for binding activity in competition experiments using native and mutant forms of the binding site; 2) These potential elements can also be mutated and tested for *in vivo* function in microinjected oocytes; 3) Internal or linker-scanning mutagenesis can be carried out to identify cis-elements not apparent by protein binding studies; and 4) Proteins could be separated on a heparin-sepharose column using a continuous KCl gradient to enhance separation of the DNA binding proteins. Binding assays using various eluted fractions could lead to the characterization of the protein(s) forming the D1 and D2 complexes.

Figure 14. Construction of the proximal and distal fragments. (A) p33B was subjected to PCR using SPK5 and SPK6 as the 5' and 3' primers respectively. The PCR product was restricted with *Hind* III and subcloned into pGEM9zf-.
(B) *Eco*R I and *Hind* III restriction of p33BHindIII-SPK6 released the proximal fragment spanning nucleotide positions -121 to +22.
(C) p33BSPK5-HindIII was restricted with *Eco*R I and *Hind* III to generate the distal fragment spanning nucleotide positions -272 to -116.

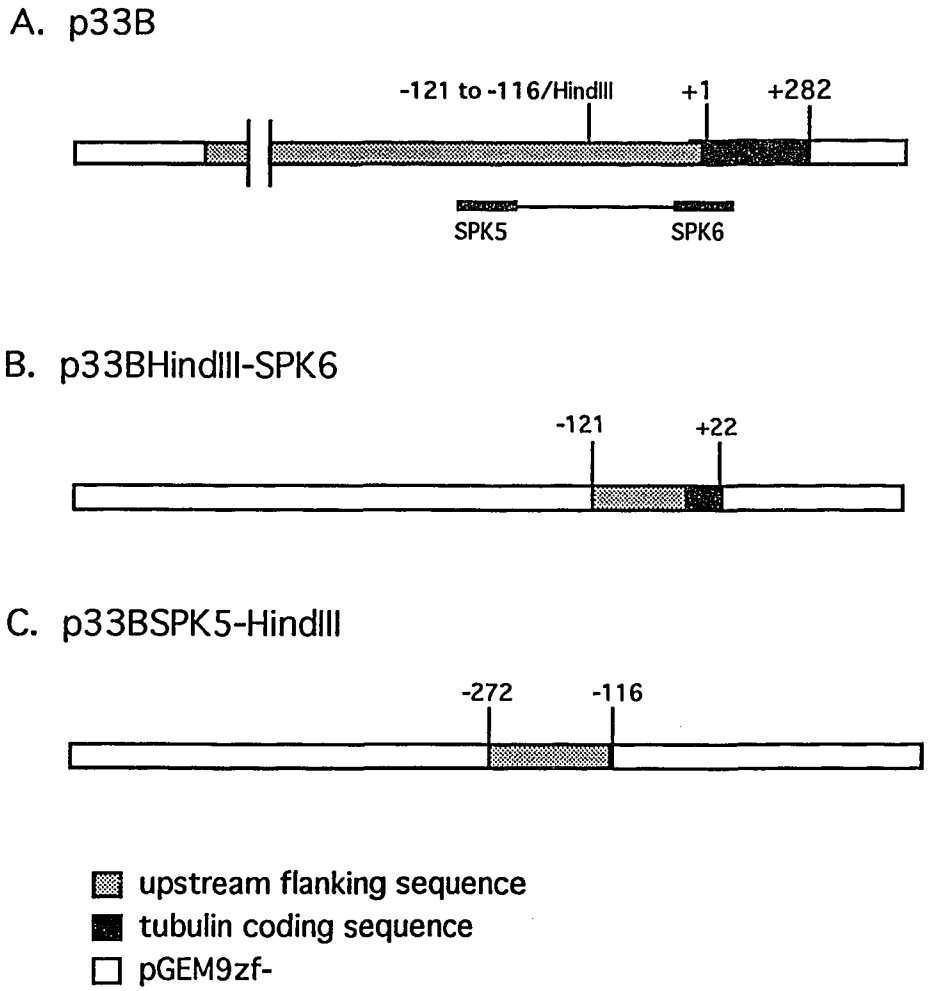

Figure 15. Gel mobility shift assays of the proximal and distal fragments with crude total ovary extracts.
The probes used in each experiment are indicated above each panel.Labelled fragments were incubated with (+) or without (-) oocyte extract. Competitors used were the proximal (p) or distal (d) fragments, as well as the 149 bp (y) and 110 bp (x) pGEM9zf-/*Msp* I fragments.
(A) Competitors are at a 200-fold molar excess. P1 and P2 identify the DNA-protein complexes.
(B) Competitors are at a 100-fold molar excess. D1 and D2 identify the DNA-protein complexes.

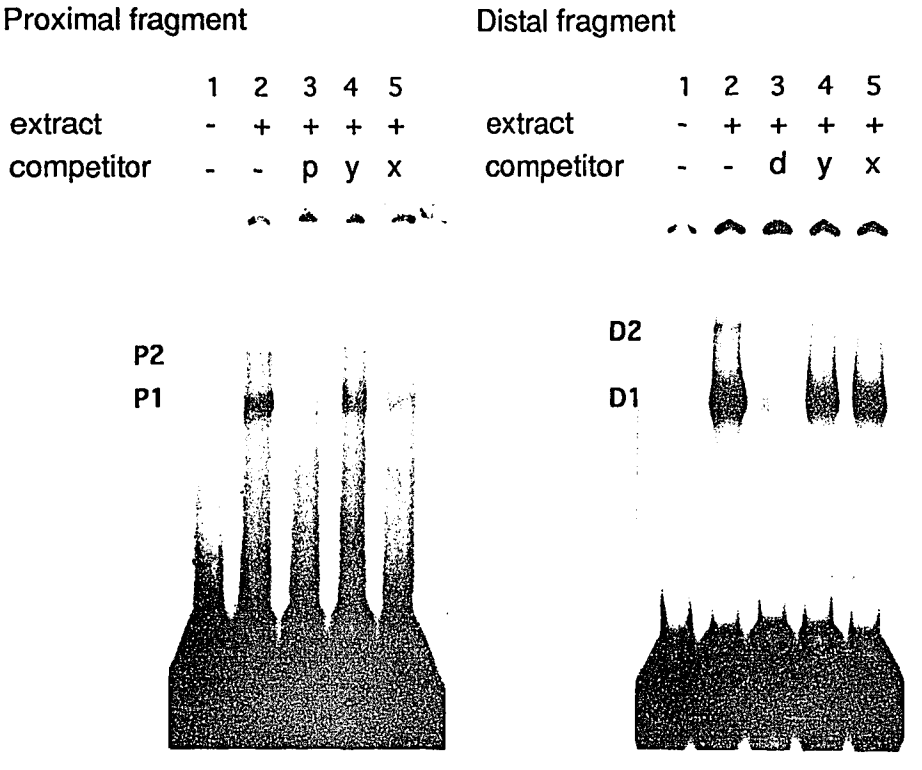

Figure 16. Competition of the proximal and distal fragments for complex formation.
Specificity of protein binding was analyzed by gel-retardation assay. Labelled distal fragment was incubated with (+) or without (-) total ovary extract. Competition was with the distal (d), proximal (p) and non-specific (y and x) fragments. D1 and D2 identify the DNA-protein complexes.

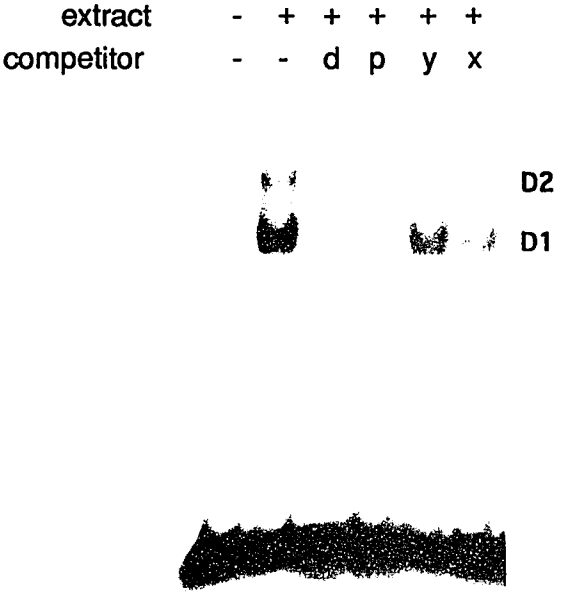

Figure 17. Competition for complex formation by the CAAT and AP2 binding sites.
The ability of oligonucleotides containing the CAAT and AP2 consensus sequences to compete with the distal fragment for complex formation (D1 and D2) was tested. Labelled distal fragment was incubated with (+) or without (-) oocyte extract in the presence of the following competitors: 120X distal fragment (lane 3), 120X NF1 (lane 4), 120X SPK7:SPK8 (lane 5), 240X NF1 (lane 6) and 240X SPK7:SPK8 (lane 7). X represents the fold-molar excess of the competitor. The NF1 oligonucleotide contains a CAAT binding site. SPK7:SPK8 contains overlapping CAAT and AP2 consensus sequences.

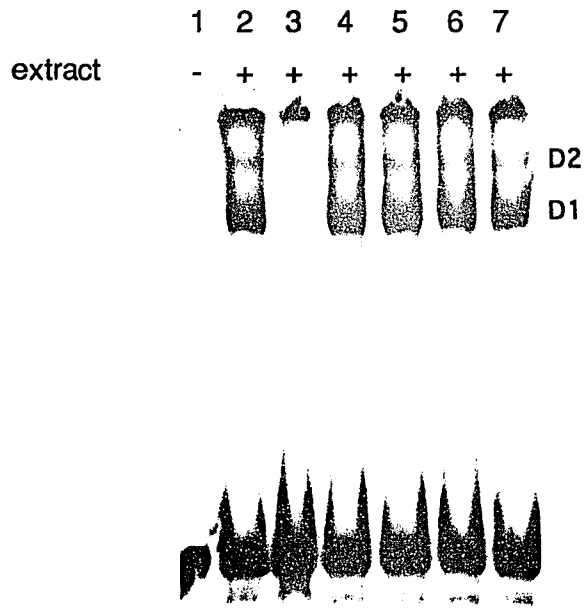

Figure 18. Kinetic analysis of complex formation. Oocyte proteins were pre-incubated with labelled distal fragment. A 200-fold molar excess of unlabelled distal fragment was then added to the reaction and aliquots were taken at 0, 1, 2, 3, 4 and 5 minutes (lanes 0-5). Lane f represents unbound probe. Lane x is a competition reaction with the non-specific competitor, fragment x. D1 and D2 identify the complexes formed.

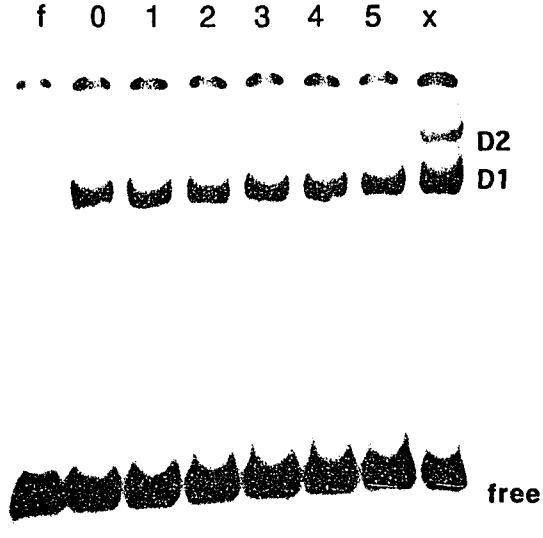

Figure 19. A comparison of complex formation by the total ovary extract and nuclear extract.
Binding activity of total ovary extracts and a nuclear extract were compared in a gel mobility-shift assay using the distal fragment as a probe. The type of extracts are indicated at the upper left of the panel. Total old and new represent different total ovary extract preparations. Protein concentrations in micrograms are noted above each lane. DNA-protein complexes are denoted by D1 and D2.

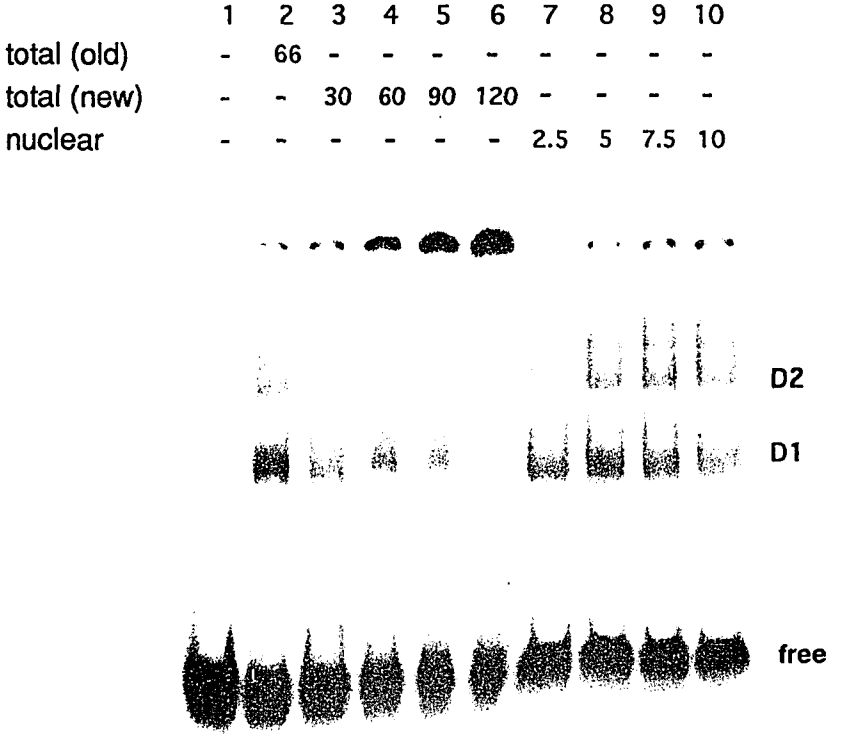

Figure 20. Gel-shift/footprint analysis of the distal fragment. The distal fragment was incubated with nuclear extract, digested with DNase I and electrophoresed on a native polyacrylamide gel. Bands corresponding to the unshifted fragment (f), and complexes D1 and D2 were extracted and electrophoresed on a 7% denaturing gel.
(A) Autoradiogram of the native gel. Portions to be extracted are as marked.
(B) Digestion pattern of the DNA obtained in A and electrophoresed on a sequencing gel.

A. Native gel

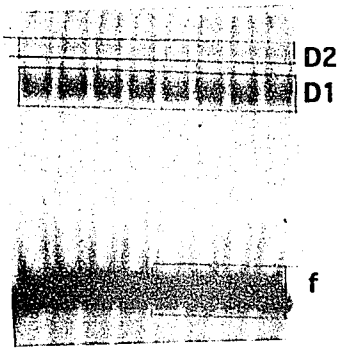

B. Sequencing gel

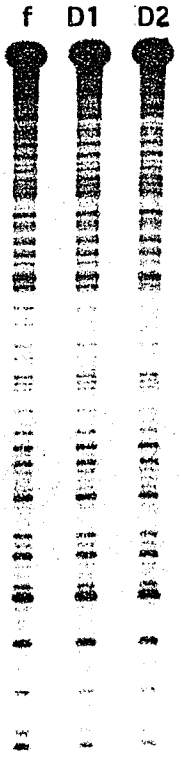

Figure 21. Gel-mobility shift assays with heparin-sepharose purified oocyte proteins.
DNA binding proteins from a total ovary extract were purified on a heparin-sepharose column and various elution fractions were tested for their ability to bind to the distal fragment. Unbound fragment (f), unpurified oocyte extract (o), 0.17M KCl wash fraction (w), fractions 7 to 13 of the 0.4M KCl elution (7-13). Complex D1 but not D2 was visible. D3 is a newly detected DNA-protein complex.
(A) Poly d(I-C) was not used in the binding reactions.
(B) Extracts were pre-incubated with 7µg poly d(I-C) prior to addition of the labelled fragment.

A. No poly d(I-C)

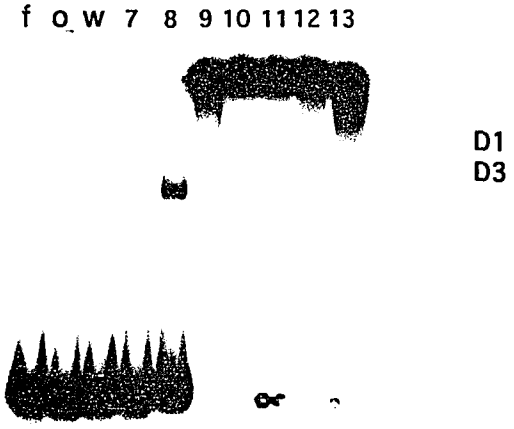

B. 7 µg poly d(I-C)

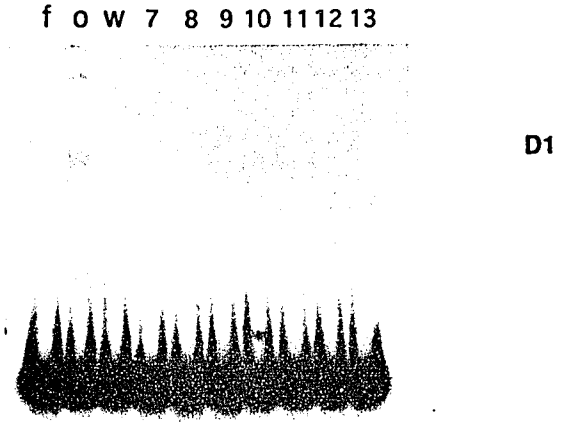

Figure 22. Titration of Poly d(I-C).
Non-specific competition by poly d(I-C) for complex formation was tested in a gel-mobility shift assay. Fraction 11 of the heparin-sepharose purification was pre-incubated with no (0), 0.5 µg (.5), 1 µg (1), or 1.5 µg (1.5) of poly d(I-C) prior to the addition of labelled distal fragment. The fragment was also incubated with no protein (f) or with unpurified oocyte extract (u) in the presence of 7 µg poly d(I-C). Only complex D1 can be detected. The faster migrating band does not correspond to complex D3.

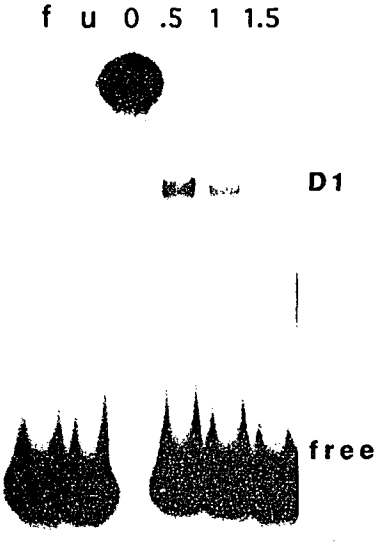

Figure 23. DNase I footprint analysis of a somatic 5S RNA gene. The 330 bp *Hind* III-*Apa* I fragment from pXls11, a somatic 5S RNA gene, was labelled on the coding strand and incubated with (lanes 1 and 2) or without (lanes 3-5) total ovary extract. The DNA was then subjected to DNase digestion for varying lengths of time (lane 1 - 2.5 min., lane 2 - 3 min., lane 3 - 1 min., lane 4 - 1.5 min., lane 5 - 2 min.). Products were analyzed on a 7% sequencing gel. The solid vertical line represents the region protected from DNase I digestion. G and A/G represent Maxam-Gilbert sequencing reactions used as markers (Maxam and Gilbert, 1980).

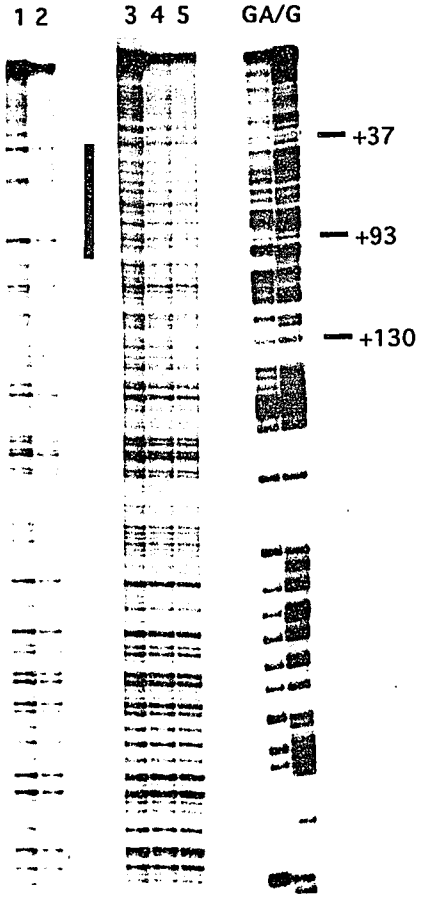

Figure 24. Summary of complex formation and potential cis-elements involved.
The 336 bp promoter region was divided into the proximal (-121 to +22) and distal (-272 to -116) fragments. Both fragments formed 2 complexes with oocyte proteins and were able to compete with each other for complex formation. The following is a summary of potential cis-elements. Sequences that are found in both fragments are centered. These four elements are also found in the human class IVb β-tubulin promoter. The subset that was tested but not found to be able to compete for complex formation are in bold. Sequences that are common to the human and frog promoters but not to the proximal and distal fragments are listed under the fragment where they can be found. Abbreviations are as follows: AP2 (AP2 binding site), CAAT (CAAT protein binding site), PEBP 1 (Polyoma enhancer binding protein 1), SV40 TAg (SV40 large T antigen binding site), 23/24 (23 of 24 bp homology specific to the human and frog class IVb β-tubulin promoters. MRE (metal responsive element from the rat metallothionein gene), SP1 (SP1 binding site).

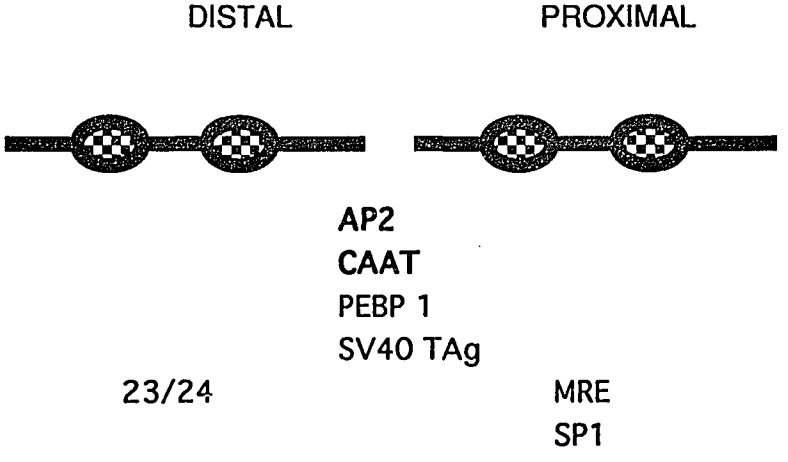

5. CO-TRANSLATIONAL AUTOREGULATION OF β-TUBULIN RNA

5.1 Introduction

The appropriate level of tubulin mRNA is established by a co-translational autoregulatory mechanism whereby mRNA stability is specified by the level of soluble tubulin. Several requirements must be met for mRNA degradation to proceed: 1) mRNA must be polysome bound; 2) Translation must be ongoing, beyond amino acid 41; and 3) The sequence Met-Arg-Glu-Ile (MREI) must be at the amino terminus of the encoded polypeptide.

β-tubulin mRNA becomes a substrate for degradation when the soluble tubulin protein concentration is elevated. Message levels of the oocyte β-tubulin variant are highest within immature oocytes and drop significantly by stage V/VI. Conversely, the level of tubulin protein increases throughout oogenesis. The inverse relationship between mRNA and protein levels implies that the autoregulatory mechanism functions in oocytes.

The oocyte system is potentially an ideal system for dissecting the components of the autoregulatory pathway. Its biggest advantage over other cell systems is that identified factors can be easily manipulated. For example, any molecule, from DNA to protein, can be microinjected into oocytes in order to inhibit or replace a particular function.

In this chapter, we describe preliminary studies aimed at determining if *Xenopus* oocytes are capable of β-tubulin autoregulation.

5.2 Results

The requirements that the β-tubulin polypeptide must encode MREI at its amino terminus and must be translated beyond codon 41 were tested. The presumed autoregulatable construct, p33B (fig. 2) contains the signal MREI and its transcript is translated beyond codon 41. The signal MREI was mutated to the non-functional sequence MVYI in the presumed non-autoregulatable construct pSal33B (Fig. 4). Translation of its transcript proceeds past codon 41. The construct p33BEcoRI-HgiAI encodes a fusion peptide whose first 5 amino acids are native to tubulin, thus the autoregulatory signal is retained; however, a stop codon is present at the ninth position, and thus the RNA should not be a substrate for autoregulation.

Three sets of oocytes in groups of 10 were injected with pSal33B, p33B or p33BEcoRI-HgiAI (fig. 25A, lanes 1-3, 4-6, and 7-9, respectively) and an equimolar amount of pH4M:HI, the histone control. Half an oocyte-equivalent of RNA was primer extended with Xlo (tubulin) or JTH4 (histone).

The result of these experiments indicate that both pSal33B and p33BEcoRI-HgiAI indeed do not yield an autoregulatable product, as transcript levels are quite high. However, level of p33B RNA is considerably lower than RNA from non-autoregulatable constructs, and similar to the background level of RNA from oocytes injected with the vector, pGEM9zf-, alone (fig. 25A, lane 10). The normalization of tubulin RNA to histone RNA indicates that there is an approximately 8- to 10-fold difference in the level of non-autoregulatable to autoregulatable β-tubulin RNA. We feel that in this case, primer extension is quantitative (section 3.2.4) as the changes in histone RNA levels parallel

changes in tubulin RNA levels within each set.

A criticism of the above study is that the histone transcription from oocytes co-injected with p33B and pH4M:HI is low. As such, one may attribute the difference in RNA levels between the autoregulatable and non-autoregulatable transcripts to a general decrease in transcription. As figure 26 shows, decreased transcription cannot account for the difference in RNA levels. p33B was dialyzed to remove all traces of cesium, which we assumed was responsible for the lowered level of expression of co-injected p33B and pH4M:HI. Four sets of oocytes in groups of 10 were injected with p33B, pSal33B or p33BEcoRI-HgiAI (lanes 1-8, 9-16 and 17-24 respectively) and pH4M:HI. Half an oocyte equivalent of RNA, in duplicate, was quantitated by primer extension.

Histone transcription was improved by dialyzing p33B indicating that cesium contamination may have had detrimental effects on the oocytes. However, we were unable to optimize transcription to the level seen when pH4M:HI is co-injected with pSal33B or p33BEcoRI-HgiAI. Nevertheless, this experiment demonstrates that the steady state level of β-tubulin RNA is depressed when the RNA contains intact autoregulatory signals (p33B). When the signal sequence is altered (pSal33B) or when translation is prematurely terminated (p33BEcoRI-HgiAI), transcript levels are elevated. In this case, the level of pSal33B and p33BEcoRI-HgiAI are 7- and 24-fold higher, respectively, than p33B RNA levels.

5.3 Discussion

The above experiments demonstrate that the co-translational autoregulatory mechanism is functional in oocytes

and is dependent on an intact amino terminal sequence and most likely, translation past codon 41. It is unclear why there is a difference in the level of the two non-autoregulatable constructs.

Several studies can be undertaken to define the nature of this autoregulatory event. First, antibodies that block the signal sequence can be microinjected into oocytes. This should inhibit autoregulation if binding of a factor to this sequence is required for RNA degradation to proceed. Similarly, an excess of peptide carrying the signal sequence can be microinjected into oocytes. This would serve as a competitor for the binding of the factor. If such is the case, this peptide in conjunction with aniti-peptide antibodies can then be used to precipitate the factor. If tubulin is the factor that binds this sequence, then the process should be blocked by injecting available anti-tubulin antibodies. Finally, total oocyte proteins can be fractionated. Reconstitution experiments can then be carried out to determine which fractions are necessary for autoregulation to proceed *in vitro*.

Figure 25. Autoregulation of tubulin RNA - 1.
Three sets of oocytes in groups of 10 were microinjected with pSal33B, an autoregulatory mutant containing the amino terminal sequence MVYI (lanes 1-3), p33B, an autoregulatable construct (lanes 4-6) or p33BEcoRI-HgiAI, a mutant that terminates translation after 8 amino acids (lanes 7-9). One set of oocytes was microinjected with pGEM9zf- alone (lane 10). pH4M:H1 was coinjected as an internal control. The expected products are indicated by a bracket and the large extended product is marked by an arrow.
(A) Tubulin RNA was primer extended with Xlo, which recognizes endogenous and plasmid-derived transcripts. However, background levels of endogenous tubulin are negligible (lane 10).
(B) Histone RNA was primer extended with JTH4.

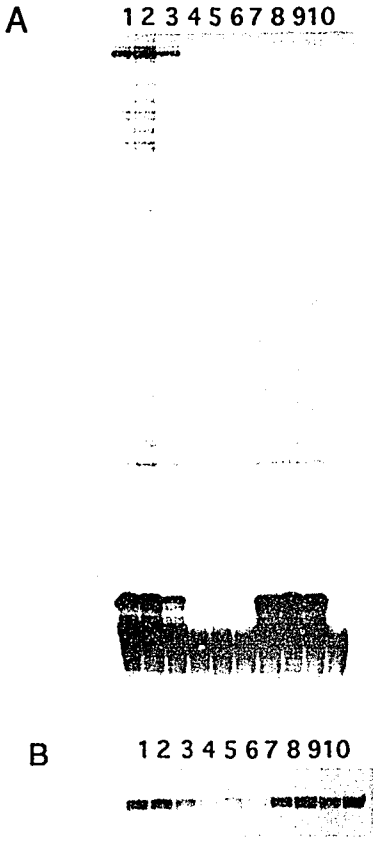

Figure 26. Autoregulation of tubulin RNA - 2.
Four sets of oocytes in groups of 10 were microinjected with p33B (lanes 1-8), pSal33B (lanes 9-16) or p33BEcoRI-HgiAI (lanes 17-24) and the internal control, pH4M:HI. One-half oocyte equivalent was assayed in duplicate by primer extension with Xlo or JTH4 (data not shown). As a control for background levels of endogenous tubulin, RNA from uninjected oocytes were primer extended with Xlo (lanes 25-26).

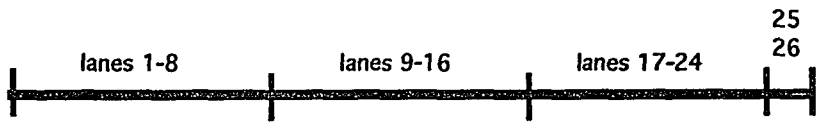

6. *XENOPUS LAEVIS* ERYTHROID β-TUBULIN

6.1 Introduction

Our laboratory has also been interested in characterizing the erythroid β-tubulin variant in *X. laevis*. This class VI member is a good model to study transcriptional regulation for two reasons: 1) Expression of class VI β-tubulins is restricted to hematopoietic tissues (Wang et al., 1986; Murphy et al., 1987). Thus, it is an ideal model for studying the regulation of erythroid specific genes; and 2) Analysis of differential regulation would be facilitated by having two tubulin genes whose expression patterns are at both extremes, ubiquitous (oocyte; section 1.11) and tissue specific (erythroid).

The mouse and chicken erythroid tubulin cDNAs have been isolated and sequenced. These divergent β-tubulins have certain characteristics that distinguish them from all other β-tubulins. Nucleic acid sequence homology to other tubulins within a species is low. For example, the chicken erythroid β-tubulin is at most 50% homologous to all other chicken tubulins. On the amino acid level, the erythroid isotypes are 83% and 78% homologous to the other chicken and mouse tubulins, respectively. Unlike other tubulins which show >90% inter-species homology within a class, the two class VI tubulins show only 82% homology to each other. The most striking region of non-homology between the two cDNAs is in the carboxy terminus, a region that typically shows conservation by isotype class across species (Table I). There are, however, 24 positions at which the conserved amino acids are unique to the erythroid proteins out of all β-tubulins (Wang et al., 1986; Murphy et al., 1987).

The erythroid tubulins form structures called marginal bands, peripheral bundles of 10-20 microtubules that lie in the plane of cellular flattening (Gambino et al., 1984). In lower vertebrates, marginal bands are only found in nucleated erythrocytes and thrombocytes.

6.2 Results

6.2.1 cDNA library screening

Two Xenopus erythroblast cDNA libraries were screened with various nucleic acid probes at lowered stringencies. The initial probe used was pT_2 (Cleveland et al., 1980), one that has been used to identify β-tubulins across isotype class and species, including the mouse erythroid variant. Since this probe did not detect any homologous β-tubulin cDNAs, we utilized pUM8, the chicken erythroid cDNA (Murphy et al., 1987). This did not detect homologous clones as well. Our inability to detect homologous sequences perhaps was not surprising since the erythroid tubulin sequence is the most divergent. In addition the region of divergence is dispersed throughout gene (Wang et al., 1986; Murphy et al., 1987).

As an alternative, we opted to use antibodies to screen a *Xenopus* erythroblast expression library. The antibodies used included two "general" anti-tubulin (Tu9A and Tu9B) and one *Bufo marinus* erythroid β-tubulin specific antibody (#62-2; D. Murphy, Johns Hopkins University). The general tubulin antibodies recognized *Xenopus* oocyte β-tubulin; however, none of the antibodies recognized the *Xenopus* erythroid β-tubulin protein. Thus, the final option was to directly isolate the *X. laevis* erythroid β-tubulin subunit and generate its own specific

antibody.

6.2.2 Purification of erythroid and oocyte β-tubulins

Erythrocytes were obtained from *Xenopus* peripheral blood and lysed in detergent to release soluble proteins while leaving the cytoskeleton, which has 75% of total cellular tubulin, intact (Murphy and Wallis, 1983). Calcium treatment in the presence of cytoplasmic factors released microtubules, which could be found in the soluble fraction after centrifugation (Gambino et al., 1985).

Xenopus oocyte tubulins were also isolated for use as size markers for the erythroid tubulins since oocyte tubulin mRNA is also expressed at low levels in erythroblasts (Bieker and Yazdani-Buicky, 1992). At least 75% of total tubulin is soluble in the oocyte (section 1.14). These were forced to polymerize with microtubule associated proteins (MAPs) in the presence of taxol (B. Suffness, NIH) and GTP. After a series of differential centrifugation steps, MAPs were subsequently removed by treatment with NaCl, resulting in purified polymeric tubulin.

Upon electrophoresis under conditions optimized to resolve tubulin subunits, two protein bands corresponding to α- and β-tubulin were detected in the oocyte extract (fig. 27, lane 2). Their localization between the 44 kd and 66 kd molecular weight markers agrees with the expected 55 kd size. In addition to α-tubulin, two erythroid tubulins are present (fig. 27, lane 3). The slower migrating of the two bands corresponds to the oocyte β-tubulin and any other non-erythroid β-tubulin variants. The fastest migrating band is erythroid β-tubulin as confirmed by microsequencing of the amino terminus (R. Kohanski, Mt. Sinai Protein Core). At the level of detection afforded by silver-

staining, the erythroid β-tubulin variant comprises ~80% of total β-tubulin protein. This is similar to chicken erythroblasts whose β-tubulin composition is ~75% erythroid-specific (Murphy et al., 1987).

6.2.3 Generation of polyclonal antibodies

Rabbit polyclonal antibody was raised against gel-purified erythroid β-tubulin as prepared above. Anti-serum from the first bleed appeared to detect a β-tubulin band on a Western blot of purified erythroid tubulin proteins. However, the results could not be reproduced even with sera from subsequent bleeds (data not shown).

6.3 Discussion

Using the above method for purification of β-tubulin polypeptides, it has since been possible to microsequence and use the information to isolate a cDNA corresponding to *Xenopus* erythroid β-tubulin. This should facilitate isolation of the genomic clone. Once available, the genomic clone can be subjected to developmental studies of tissue specificity. For example, cis-acting elements responsible for correct temporal and spatial expression can be monitored during embryogenesis by microinjection of a reporter gene driven by the erythroid tubulin promoter, into unfertilized eggs. Finally, trans-activating factors present in *Xenopus* erythroid cells that bind to these sequences can be determined.

Figure 27. Separation of *Xenopus laevis* oocyte α- and β-tubulins.
Purified oocyte (lane 2) and erythroid (lane 3) tubulins were electrophoresed on a 6% SDS-polyacrylamide gel and visualized by silver staining. A single α-tubulin band representing a mixture of all expressed α-tubulins is present in both extracts. The oocyte extract has one β-tubulin band representing at least one isotype (*Xlot*), possibly two (Bieker and Yazdani-Buicky, 1992). There are at least two β-tubulin proteins in erythroid cells. The erythroid variant comprises most of the protein pool while the oocyte isotype is a minor component. Molecular weight markers (lane 1) are as indicated.

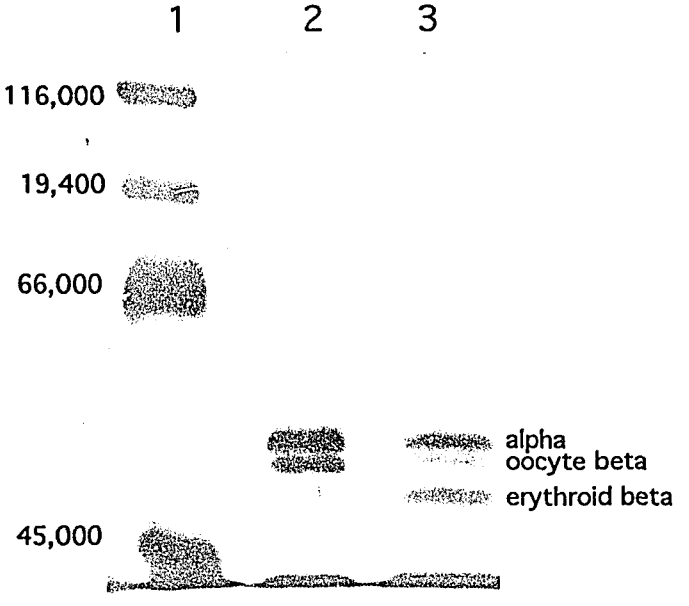

7. DISCUSSION

Microtubules, comprised of α- and β-tubulin heterodimers, form diverse structures with a wide range of functions. This versatility is controlled in part by the ratio of functionally distinct β-tubulin isovariants expressed within a cell. The proper level of each expressed isotype is controlled by two mechanisms, on the nucleic acid level: 1) Tubulin mRNA is degraded co-translationally, in response to the level of soluble tubulin heterodimers; and 2) Differential regulation of various promoters serves to control the expression level of members of the β-tubulin gene family.

We have begun characterization of the *Xenopus laevis* oocyte β-tubulin (*Xlot*) gene. This is classified as a class IVb tubulin based on its carboxy terminus and tissue distribution. *Xlot* is expressed ubiquitously at low levels. Expression is significantly higher in germ-cells.

Preliminary studies aimed at determining whether oocytes regulate tubulin RNA levels co-translationally indicate that the autoregulatory mechanism is at work. The level of tubulin RNA from a construct containing the appropriate autoregulatory characteristics (MREI at the amino terminus; no stop codons before residue 41) appears to be at least 7-fold lower than RNA from a construct with the non-functional sequence, MVYI, or one with a stop codon at position 9.

Transcriptionally, the *Xlot* promoter appears to be quite strong, as CAT activity derived from a chimeric Xlot-CAT fusion is comparable to that from pBLCAT2, which is known to be a very strong promoter. It was further shown that transcriptional

activity derived from a 336 bp promoter region was half that derived from a 1400 bp promoter construct. Sequence analysis of this limited region reveals numerous potential cis-acting elements. However, very few tubulin promoters have been sequenced, and none have been characterized. Thus detailed comparisons to other tubulin promoters cannot be made.

The 336 bp region has been analyzed by deletion mutagenesis and protein binding studies. Results from such experiments and sequence comparison of the human and frog class IVb promoters highlight some potential cis-elements.

The first 177 bp upstream of the transcription start site can be considered a minimal promoter which, at most, drives 2% of activity compared to the 1400 bp promoter. Sequence analysis shows that a TATA box can be found at -30 and a CAAT box at -87. By definition, this is a typical RNA Polymerase II-transcribed promoter. Additionally, a DNA fragment encompassing most of this region (proximal fragment) forms two complexes with oocyte proteins. The region between positions -177 and -227 (distal fragment) contains almost all the activity driven by the 336 bp promoter region. The distal fragment also forms two complexes with oocyte proteins.

Interestingly, the complexes formed with the distal fragment can be competed by the proximal fragment. One is therefore led to believe that elements common to both fragments are responsible for the DNA-protein complexes observed. Sequence analysis shows that both fragments contain the following consensus sequences: 1) CAAT protein binding site; 2) AP2 binding site; 3) Polyoma enhancer binding protein 1 binding site; and 4) SV40 large T antigen binding site. These

potential elements are common not only to the two fragments but to the human class IVb β-tubulin promoter as well. Two of these elements were tested for binding activity.

Of the known cis-elements, the CAAT consensus is the best candidate to be a functional element. It is found 5 and 4 times in the frog and human class IVb promoters, respectively. CAAT proteins are also ubiquitous and deletion of the CAAT sequence inhibits transcription of certain genes in oocytes. Surprisingly, two oligonucleotides containing the CAAT consensus do not compete for complex formation with the distal fragment. Either a CAAT-binding protein is not involved in *Xlot* transcription, or there is another CAAT protein that does not bind to the two oligonucleotides tested.

The second candidate is AP2 as it is present once within each fragment. We were not able to demonstrate competition by an AP2-containing oligonucleotide for complex formation with the distal fragment, a result that supports the finding that the RNA coding for the *Xenopus* homologue to the human AP2 protein is not expressed in oocytes.

The third candidate for complex formation is the 23/24 bp region of homology between the human and frog promoters. It is found only in the distal fragment, in a region that appears to be functionally insignificant. However, this sequence is found in identical regions in both promoters and is not found in any other promoter. If it is a functional element, deletion of a second element of opposite function may have masked its existence. In addition a smaller sequence within may serve as a core consensus shared with other promoters. The remainder of the sequence may function in specificity as with the CAAT protein binding sites.

Since *Xlot* is expressed in oocytes at higher levels

compared to all other tissues, one may expect to find oocyte-specific DNA motifs or oocyte-specific activators. Since α- and β-tubulins are found at the same level in all cells, one may also expect to find an α-tubulin expressed in a similar pattern to *Xlot*. The *Xenopus* α-tubulin *XαT14* is expressed at high levels in oocytes and at low levels in a range of cell types, similar to *Xlot* (Middleton and Morgan, 1989). It is unlike *Xlot* in that expression is low in testis. A comparison of the *XαT14* and *Xlot* promoters reveals some differences and similarities. *XαT14* has a heat shock element-like sequence responsible for about 60% of promoter activity. The sequence is not present in the first 600 bp of the *Xlot* promoter. On the other hand, *XαT14* has three CAAT boxes and *Xlot* has four. It is possible that an oocyte CAAT-like binding protein is responsible for the activity of oocyte specific or upregulated genes.

Xlot is an ideal model to study transcriptional regulation because it is ubiquitously expressed but is also upregulated in a tissue-specific manner (germ-cells). First, an understanding of regulatory events in oocytes may shed some light on the regulation of germ-cell specific genes. Second, it is possible that the general tubulins are regulated such that a selected β-tubulin isotype can be highly expressed along with a block of genes at a particular time in development and/or in a tissue specific manner. Upregulated *Xlot* expression may be specifically required during germ-cell differentiation, for example, to provide large amounts of stored tubulin protein in the oocyte for later use during early development. This would provide a strong example of the isotubulin hypothesis (section 1.6). Further characterization of the *Xlot* and other germ-cell

promoters will shed light on whether its upregulation is coincidental with a set of genes in the oocyte whose expression is important for the oocyte's role as a reservoir of enzymes and structural proteins.

8. BIBLIOGRAPHY

Ahmad, S., Singh, B. and Gupta, R. S. (1991). Nucleotide sequences of three different isoforms of beta-tubulin cDNA from Chinese Hamster Ovary cells. Biochim. Biophys. Acta. 1090, 252-254.

Al-Mukhtar, K. A. K. and Webb, A. C. (1971). An ultrastructural study of primordial germ cells, oogonia and early oocytes in *Xenopus laevis*. J. Embryol. Exp. Morph. 26, 195-217.

Asai, D. J. and Remolona, N. M. (1989). Tubulin isotype usage in vivo: a unique spatial distribution of the minor neuronal-specific beta-tubulin isotype in pheochromocytoma cells. Dev. Biol. 132, 398-409.

Ben-Ze'ev, A., Farmer, S. R. and Penman, S. (1979). Mechanisms of regulating tubulin synthesis in cultured mammalian cells. Cell 17, 319-325.

Bialojan, S., Falkenburg, D. and Renkawitz-Pohl, R. (1984). Characterization and developmental expression of beta-tubulin genes in *Drosophila melanogaster*. EMBO J 3, 2543-2548.

Bieker, J. J. and Yazdani-Buicky, M. (1992). The multiple beta-tubulin genes of *Xenopus*: Isolation and developmental expression of a germ-cell isotype beta-tubulin gene. Differentiation 50, 15-23.

Binder, L. I., Frankfurter, A. and Rebhun, L. I. (1985). The distribution of tau in the mammalian central nervous system. J. Cell Biol. 101, 1371-1378.

Bond, J. F., Fridovich-Keil, J. L., Pillus, L., Mulligan, R. C. and Solomon, F. (1986). A chicken yeast chimeric beta-tubulin protein is incorporated into mouse microtubules in vivo. Cell 44, 461-468

Boshart, M., Kluppel, M., Schmidt, A., Schutz, G. and Luckow, B. (1992). Reporter constructs with low background activity

utilizing the *cat* gene. Gene 110, 129-130.

Bradford, M. M. (1976). A rapid and sensitive method for the quantitation of microgram quantities of protein utilizing the principle of protein-dye binding. Anal. Biochem. 72, 248-254.

Bruhat, A., Tourmente, S., Chapel, S., Sobrier, M. L., Couderc, J. L. and Dastugue, B. (1990). Regulatory elements in the first intron contribue to transcriptional regulation of the ß3 tubulin gene by 20-hydroxyecdysone in *Drosophila* Kc cells. Nuc. Acids Res. 18, 2861-2867.

Burgoyne, R. D., Cambray-Deakin, M. A., Lewis, S. A., Sarkar, S. and Cowan, N. J. (1988). Differential distribution of beta-tubulin isotypes in cerebellum. EMBO J 7, 2311-2319.

Burnette, W. N. (1981). "Western blotting": Electrophoretic transfer of proteins from sodium dodecyl sulfate-polyacrylamide gels to unmodified nitrocellulose and radiographic detection with antibody and radioiodinated protein A. Anal. Biochem. 112, 195-203.

Burns, R. G. and Surridge, C. (1990). Analysis of beta-tubulin sequences reveals highly conserved, coordinated amino acid substitutions. Evidence that these "hot spots" are directly involved in the conformational change required for dynamic instability. FEBS Lett. 271, 1-8.

Carlier, M.-F., Hill, T. L. and Chen, Y.-D. (1984). Interference of GTP hydrolysis in the mechanism of microtubule assembly: an experimental study. Proc. Natl. Acad. Sci. USA 81, 771-775.

Chene, P., Mazarguil, H. and Wright, M. (1992). Microtubule assembly protects the region 28-38 of the beta-tubulin subunit. Cell. Motil. Cytoskeleton 22, 25-37.

Chodosh, L. A., Baldwin, A. S., Carthew, R. W. and Sharp, P. A. (1988). Human CCAAT-binding proteins have heterologous subunits. Cell 53, 11-24.

Cleveland, D. W. and Havercroft, J. C. (1983). Is apparent autoregulatory control of tubulin synthesis nontranscriptionally regulated? J. Cell. Biol. 97, 919-924.

Cleveland, D. W., Lopata, M. A., MacDonald, R. J., Cowan, N. J., Rutter, W. J. and Kirschner, M. W. (1980). Number and evolutionary conservation of alpha- and beta-tubulin and cytoplasmic beta- and gamma-actin genes using specific cloned cDNA probes. Cell 20, 95-105.

Cleveland, D. W., Lopata, M. A., Sherline, P. and Kirschner, M. W. (1981). Unpolymerized tubulin modulates the level of tubulin mRNAs. Cell 25, 537-546.

Cohen, W. D. and Ginsburg, M. F. (1986). Isolation of the erythrocyte marginal band. Methods Enzymol. 134, 232-252.

Cross, D., Dominguez, J., Maccioni, R. B. and Avila, J. (1991). MAP-1 and MAP-2 binding sites at the C-terminus of beta-tubulin. Studies with synthetic peptides. Biochemistry 30, 4362-4366.

Currie, D. and Bate, M. (1991). The development of adult abdominal muscles in *Drosophila*: myoblasts express twist and are associated with nerves. Development 113, 91-102.

Dabora, S. L. and Sheetz, M. P. (1988). The microtubule-dependent formation of a tubulovesicular network with characteristics of the ER from cultured cell extracts. Cell 54, 27-35.

Davidson, E. H. (1986). Gene activity in early development. Academic Press, Inc., Orlando.

Dolecki, G. V. and Smith, L. D. (1979). Poly (A)+ RNA metabolism during oogenesis in *Xenopus laevis*. Dev. Biol. 69, 217-236.

Drubin, D. G. and Kirschner, M. W. (1986). Tau protein function in living cells. J. Cell Biol. 103, 2739-2746.

Dumont, J. N. (1972). Oogenesis in *Xenopus laevis* (Daudin). I. Stages of oocyte development in laboratory maintained animals.

J. Morph. 136, 153-180.

Dworkin-Rastl, E., Kelley, D. B. and Dworkin, M. B. (1986). Localization of specific mRNA sequences in *Xenopus laevis* embryos by in situ hybridization. J. Embryol. Exp. Morphol. 91, 153-168.

Edde, B., Rossier, J., Le Caer, J. P., Desbruyeres, E., Gros, F. and Denoulet, P. (1990). Posttranslational glutamylation of alpha-tubulin. Science 247, 83-83.

Engelborghs, Y., Mertens, K., Willaert, K., Luan-Rilliet, Y. and Cox, J. A. (1990). Kinetics of conformational changes in *Nereis* sarcoplasmic calcium-binding protein upon binding of divalent cations. J. Biol. Chem. 265, 1809-1815.

Engelke, D. R., Ng, S.-Y., Shastry, B. S. and Roeder, R. G. (1980). Specific interaction of a purified transcription factor with an internal control region of 5S RNA genes. Cell 19, 717-728.

Falconer, M. M., Echeverri, C. J. and Brown, D. L. (1992). Differential sorting of beta-tubulin isotypes into colchicine-stable microtubules during neuronal and muscle differentiation of embryonal carcinoma cells. Cell. Motil. Cytoskeleton 21, 313-325.

Feick, P., Foisner, R. and Wiche, G. (1991). Immunolocalization and molecular properties of a high molecular weight microtubule-bundling protein (syncolin) from chicken erythrocytes. J. Cell Biol. 112, 689-699.

Fuller, M. T., Caulton, J. H., Hutchens, J. A., Kaufman, T. C. and Raff, E. C. (1988). Mutations that encode partially functional beta2 tubulin subunits have different effects on structurally different microtubule arrays. J. Cell Biol. 107, 141-152.

Fulton, C. and Simpson, P. A. (1976). Selective synthesis and utilization of flagellar tubulin. The multitubulin hypothesis. In "Cell Motility" (Goldman, R., Pollard, T. and Rosenbaum, J., Ed.), pp. 978-1005. Cold Spring Harbor Laboratory, Cold Spring Harbor.

Galas, D. and Schmitz, A. (1978). DNase footprinting: a simple method for the detection of protein-DNA binding specificity. Nucl. Acids Res. 5, 3157-3170.

Gambino, J., Ross, M. J., Weatherbee, J. A., Gavin, R. H. and Eckhardt, R. A. (1985). *Xenopus* marginal band disassembly by calcium-activated cytoplasmic factors. J. Cell Sci. 79, 199-215.

Gambino, J., Weatherbee, J. A., Gavin, R. H. and Eckhardt, R. A. (1984). Studies on the cytoskeletal and nuclear architecture of *Xenopus* erythrocytes. J. Cell Sci. 72, 275-294.

Gard, D. L. (1991). Organization, nucleation, and acetylation of microtubules in *Xenopus laevis* oocytes: a study by confocal immunofluorescence microscopy. Dev. Biol. 143, 346-362.

Gard, D. L. and Kirschner, M. W. (1987). Microtubule assembly in cytoplasmic extracts of *Xenopus* oocytes and eggs. J. Cell Biol. 105, 2191-2201.

Garner, M. M. and Revzin, A. (1981). A gel electrophoresis method for quantifying the binding of proteins to specific DNA regions. Applications to components of the E. coli lactose operon regulatory system. Nucl. Acis Res. 9, 3047-3060.

Gasch, A., Hinz, U., Leiss, D. and Renkawitz-Pohl, R. (1988). The expression of beta1 and beta3 tubulin genes of *Drosophila melanogaster* is spatially regulated during embryogenesis. Mol. Gen. Genet. 211, 8-16.

Gasch, A., Hinz, U. and Renkawitz-Pohl, R. (1989). Intron and upstream sequences regulate expression of the Drosophila ß3-tubulin gene in the visceral and somatic musculature, respectively. Proc. Natl. Acad. Sci. USA 86, 3215-3218.

Gay, D. A., Sisodia, S. S. and Cleveland, D. W. (1989). Autoregulatory control of beta-tubulin mRNA is linked to translation elongation. Proc. Natl. Acad. Sci. USA 86, 5763-5767.

Gay, D. A., Yen, T. J., Lau, J. T. Y. and Cleveland, D. W. (1987). Sequences that confer beta-tubulin autoregulation through

modulated mRNA stability reside within exon 1 of a beta-tubulin mRNA. Cell 50, 671-679.

Gelles, J., Schnapp, B. J. and Sheetz, M. P. (1988). Tracking kinesin-driven movements with nanometre-scale precision. Nature 331, 450-453.

Golden, L., Schafer, U. and Rosbash, M. (1980). Accumulation of individual pA+ RNAs during oogenesis of *Xenopus laevis*. Cell 22, 835-844.

Goldin, A. (1992). Maintenance of Xenopus laevis and oocyte injection. Methods Enzymol. 207, 266-279.

Good, P. J., Richter, K. and Dawid, I. B. (1989). The sequence of a nervous system-specific, class II beta-tubulin gene from *Xenopus laevis*. Nucl. Acids Res. 17, 1000.

Gorman, C. M., Moffat, L. F. and Howard, B. H. (1982). Recombinant genomes which express chloramphenicol acetyl transferase in mammalian cells. Mol. Cell. Biol. 2, 1044-1051.

Gundersen, G. G. and Bulinski, J. C. (1986). Distribution of tyrosinated and non-tyrosinated alpha-tubulin during mitosis. J. Cell Biol. 102, 1118-1126.

Gurdon, J. B. and Wickens, M. P. (1983). The use of *Xenopus* oocytes for the expression of cloned genes. Methods Enzymol. 101, 370-386.

Havercroft, J. C. and Cleveland, D. W. (1984). Programmed expression of beta-tubulin genes during development and differentiation of the chicken. J. Cell Biol. 99, 1927-1935.

Hecht, N. B., Distel, R. J., Yelick, P. C., Tanhauser, S. M., Driscoll, C. E., Goldberg, E. and Tung, K. S. K. (1988). Localization of a highly divergent mammalian testicular alpha-tubulin that is not detectable in brain. Mol. Cell. Biol. 8, 996-1000.

Heidemann, S. R., Hamborg, M. A., Balasz, J. E. and Lindley, S.

(1985). Microtubules in immature oocytes of *Xenopus laevis*. J. Cell Sci. 77, 129-141.

Hill, R. S. (1979). A quantitative electron-microscope analysis of chromatin from *Xenopus laevis* lampbrush chromosomes. J. Cell Sci. 40, 145-169.

Hinz, U., Wolk, A. and Renkawitz-Pohl, R. (1992). *Ultrabithorax* is a regulator of beta3 tubulin expression in the *Drosophila* visceral mesoderm. Development 116, 543-554.

Hirokawa, N., Takemura, R. and Hisanaga, S.-I. (1985). Cytoskeletal architecture of isolated mitotic spindle with special reference to microtubule associated proteins and cytoplasmic dynein. J. Cell Biol. 101, 1858-1870.

Hoffman, P. N. and Cleveland, D. W. (1988). Neurofilament and tubulin expression recapitulates the developmental program during axonal regeneration: induction of a specific beta-tubulin isotype. Proc. Natl. Acad. Sci. USA 85, 4530-4533.

Holwill, S., Haesman, J., Crawley, C. R. and Wylie, C. C. (1987). Axis and germ line deficiencies caused by u.v. irradiation of *Xenopus* oocytes cultured in vitro. Development 100, 735-743.

Hoyle, H. D. and Raff, E. C. (1990). Two *drosophila* beta-tubulin isoforms are not functionally equivalent. J. Cell. Biol. 111, 1009-1026.

Ikeda, Y. and Steiner, M. (1978). Sulfhydryls of platelet tubulin: their role in polymerization and colchicine binding. Biochemistry 17, 3454-3459.

Jessus, C., Thibier, C. and Ozon, R. (1985). Identification of microtubule-associated proteins (MAPs) in *Xenopus* oocyte. FEBS Letters 192, 135-140.

Jessus, C., Thibier, C. and Ozon, R. (1987). Levels of microtubules during meiotic maturation of the *Xenopus* oocyte. J. Cell Sci. 87, 705-712.

Joshi, H. C. and Cleveland, D. W. (1989). Differential utilization of beta-tubulin isotypes in differentiating neurites. J. Cell. Biol. 109, 663-673.

Joshi, H. C., Yen, T. J. and Cleveland, D. W. (1987). In vivo coassembly of a divergent ß-tubulin subunit (cß6) into microtubules of different function. J. Cell Biol. 105, 2179-2190.

Kunkel, T. A., Roberts, J. D. and Zakour, R. A. (1987). Rapid and efficient mutagenesis without phenotypic selection. Methods Enzymol. 154, 367-382.

Laemmli, U. K. (1970). Cleavage of structural proteins during the assembly of the head of the bacteriophage T4. Nature 227, 680-685.

Lee, M. K., Tuttle, J. B., Rebhun, L. I., Cleveland, D. W. and Frankfurter, A. (1989). The expression and posttranslational modification of a neuron-specific beta-tubulin isotype during chick embryogenesis. Cell. Motil. Cytoskeleton 17, 118-132.

Leiss, D., Hinz, U., Gasch, A., Mertz, R. and Renkawitz-Pohl, R. (1988). Beta3 tubulin expression characterizes the differentiating mesodermal germ layer during *Drosophila* embryogenesis. Development 104, 525-531.

Lewis, S. A. and Cowan, N. J. (1988). Complex regulation and functional versatility of mammalian alpha- and beta-tubulin isotypes during the differentiation of testis and muscle cells. J. Cell. Biol. 106, 2023-2033.

Lewis, S. A., Gilmartin, M. E., Hall, J. L. and Cowan, N. J. (1985). Three expressed sequences within the human ß-tubulin multigene family each define a distinct isotype. J. Mol. Biol. 182, 11-20.

Lewis, S. A., Gu, W. and Cowan, N. J. (1987). Free intermingling of mammalian ß-tubulin isotypes among functionally distinct microtubules. Cell 49, 539-548.

Linse, K. and Mandelkow, E.-M. (1988). The GTP-binding peptide

of beta-tubulin. Localization by direct photoaffinity labeling and comparison with nucleotide-binding proteins. J. Biol. Chem. 263, 15205-15210.

Littauer, U. Z., Giveon, D., Thierauf, M., Ginzburg, I. and Ponstingl, H. (1986). Common and distinct tubulin binding sites for microtubule-associated proteins. Proc. Natl. Acad. Sci. USA 83, 7162-7166.

Little, M. and Luduena, R. F. (1985). Structural differences between beta1- and beta2-tubulins: implications for microtubule assembly and colchicine binding. EMBO J 4, 52-56.

Little, M. and Seehaus, T. (1988). Comparative analysis of tubulin sequences. Comp. Biochem. Physiol. 90, 655-670.

Lopata, M. A. and Cleveland, D. W. (1987). In vivo microtubules are copolymers of available ß-tubulin isotypes: localization of each of six vertebrate ß-tubulin isotypes using polyclonal antibodies elicited by synthetic peptide antigens. J. Cell Biol. 105, 1707-1720.

Luckow, B. and Schutz, G. (1987). CAT constructions with multiple unique restriction sites for the functional analysis of eukaryotic promoters and regulatory elements. Nucl. Acids Res. 15, 5490.

Luduena, R. F. and Roach, M. C. (1991). Tubulin sulfhydryl groups as probes and targets for anti-mitotic and antimicrotubule agents. Pharmacol. Ther. 49, 133-152.

Luduena, R. F., Roach, M. C., Trcka, P. P., Little, M., Palanivelu, P., Binkley, P. and Prasad, V. (1982). Beta2-tubulin, a form of chordate brain tubulin with lesser reactivity toward an assembly-inhibiting sulfhydryl-directed cross-linking reagent. Biochemistry 21, 4787-4794.

Matsuzaki, F., Harada, F., Nabeshima, Y., Fujii-Kuriyama, Y. and Yahara, I. (1987). Cloning of cDNAs for two beta-tubulin isotypes expressed in murine T cell lymphoma, L5178Y and analysis of their translation products. Cell Struct. Funct. 12, 317-325.

McKnight, S. and Gavis, E. R. (1980). Expression of the herpes thymidine kinase gene in Xenopus laevis oocytes: an assay for the study of deletion mutants constructed in vitro. Nucl. Acids Res. 8, 5931-5948.

Mejillano, M. R. and Himes, R. H. (1991). Assembly properties of tubulin after carboxyl group modification. J. Biol. Chem. 266, 657-664.

Michiels, F., Falkenburg, D., Muller, A. M., Hinz, U., Otto, U., Bellmann, R., Glatzer, K. J., Brand, R., Bialojan, S. and Renkawitz-Pohl, R. (1987). Testis-specific beta2 tubulins are identical in *Drosophila melanogaster* and *D. hydei* but differ from the ubiquitous beta1 tubulin. Chromosoma 95, 387-395.

Michiels, F., Gasch, A., Kaltschmidt, B. and Renkawitz-Pohl, R. (1989). A 14 bp promoter element directs the testis specificity of the Drosophila ß2 tubulin gene. EMBO J. 8, 1559-1565.

Middleton, K. and Morgan, G. T. (1989). An oocyte-expressed alpha-tubulin gene in Xenopus laevis; sequences required for the initiation of transcription. Nucl. Acids Res. 17, 5041-5055.

Miller, O. L. and Bakken, A. H. (1972). Morphological studies of transcription. Acta Endocrinol. (Copenhagen) 168, 155-177.

Mitchell, P. J. and Tijan, R. (1989). Transcriptional regulation in mammalian cells by sequence-specific DNA binding proteins. Science 245, 371-378.

Mohun, T. J., Brennan, S., Dathan, N., Fairman, S. and Gurdon, J. B. (1984). Cell type-specific activation of actin genes in the early amphibian embryo. Nature 311, 716-721.

Moskowitz, P. F., Smith, R., Pickett, J., Frankfurter, A. and Oblinger, M. M. (1993). Expression of the class III beta-tubulin gene during axonal regeneration of rat dorsal root ganglion neurons. J. Neurosci. Res. 34, 129-134.

Murphy, D. B. and Wallis, K. T. (1983). Isolation of microtubule

protein from chicken erythrocytes and determination of the critical concentration for tubulin polymerization in vitro and in vivo. J. Biol. Chem. 258, 8357-8364.

Murphy, D. B., Wallis, K. T., Machlin, P. S., Ratrie III, H. and Cleveland, D. W. (1987). The sequence and expression of the divergent beta-tubulin in chicken erythrocytes. J. Biol. Chem. 262, 14305-14312.

Natzle, J. E. and McCarthy, B. J. (1984). Regulation of *Drosophila* alpha and beta tubulin genes during development. Dev. Biol. 104, 187-198.

Neve, R. L., Harris, P., Kosik, K. S., Kumit, D. M. and Donlon, T. A. (1986). Identification of cDNA clones for the human microtubule-associated protein tau and chromosomal localization of the genes for tau and microtubule associated protein 2. Brain Res. 387, 271-280.

Oakley, B. R., Oakley, C. E., Yoon, Y. and Jung, M. K. (1990). Gamma-tubulin is a component of the spindle pole body that is essential for microtubule function in *Aspergillus nidulans*. Cell 61, 1289-1301.

Oakley, C. E. and Oakley, B. R. (1989). Identification of gamma-tubulin, a new member of the tubulin superfamily encoded by *mipA* gene of *Aspergillus nidulans*. Nature 338, 662-664.

Ovsenek, N. and Heikkila, J. J. (1990). DNA sequence-specific binding activity of the heat shock transcription factor is heat-inducible before the midblastula transition of early *Xenopus* development. Development 110, 427-433.

Pachter, J. S., Yen, T. J. and Cleveland, D. W. (1987). Autoregulation of tubulin expression is achieved through specific degradation of polysomal tubulin mRNAs. Cell 51, 283-292.

Pestell, R. Q. W. (1975). Microtubule protein synthesis during oogenesis and early embryogenesis in Xenopus laevis. Biochem. J. 145, 527-534.

Peterson, R. C., Doering, J. L. and Brown, D. D. (1980). Characterization of two Xenopus somatic 5S DNAs and one minor oocyte-specific 5S DNA. Cell 20, 131-141.

Piperno, G., Ledizet, M. and Chang, X. J. (1987). Microtubules containing acetylated alpha-tubulin in mammalian cells in culture. J. Cell Biol. 104, 289-302.

Ponstingl, H., Krauhs, E., Little, M., Kempf, T. and Hofer, T. (1981). Complete amino acid sequence of alpha and beta tubulin from procine brain: heterogeneity and regional similarity to muscle proteins. Proc. Natl. Acad. Sci. USA 78, 2757-2767.

Pratt, L. F. and Cleveland, D. W. (1988). A survey of the alpha-tubulin gene family in chicken: unexpected sequence heterogeneity in the polypeptides encoded by five expressed genes. EMBO J 7, 931-940.

Pratt, L. F., Okamura, S. and Cleveland, D. W. (1987). A divergent testis-specific alpha-tubulin isotype that does not contain a coded C-terminal tyrosine. Mol. Cell. Biol. 7, 552-555.

Prescott, A. R., Foster, K. E., Warn, R. M. and Gull, K. (1989). Incorporation of tubulin from an evolutionarily diverse source, *Physarum polycephalum*, into microtubules of a mammalian cell. J. Cell Sci. 92, 595-605.

Probst, E., Kressman, A. and Birnstiel, M. L. (1979). Expression of sea urchin histone genes in the oocyte of *Xenopus laevis*. J. Mol. Biol. 135, 709-732.

Raff, E. C. (1984). Genetics of microtubule systems. J. Cell Biol. 99, 1-10.

Raff, E. C., Diaz, H. B., Hoyle, H. D., Hutchens, J. A., Kimble, M., Raff, R. A., Rudolph, J. E. and Subler, M. A. (1987). Origin of multiple gene families: are there both functional and regulatory constraints? In "Development as an Evolutionary Process" (Raff, R. A. and Raff, E. C., Ed.), pp. 203-238. Alan R. Liss, Inc., New York.

Renthal, R., Schneider, B. G., Miller, M. M. and Luduena, R. F. (1993).

Beta IV is the major beta-tubulin isotype in bovine cilia. Cell Motil. Cytoskeleton

Richter, J. D., Anderson, D. M., Davidson, E. H. and Smith, L. D. (1984). Interspersed poly(A) RNAs of amphibian oocytes are not translatable. J. Mol. Biol. 173, 227-241.

Richter, K., Grunz, H. and Dawid, I. B. (1988). Gene expression in the embryonic nervous system of *Xenopus laevis*. Proc. Natl. Acad. Sci. USA 85, 8086-8090.

Roeder, R. G. (1974). Multiple forms of deoxyribonucleic acid-dependent ribonucleic acid polymerase in *Xenopus laevis*. J. Biol. Chem. 249, 249-256.

Rosenfeld, P. J., O'Neill, E. A., Wides, R. J. and Kelly, T. J. (1987). Sequence-specific interactions between cellular DNA-binding proteins and the adenovirus origin of DNA replication. Mol. Cell. Biol. 7, 875-886.

Rudolph, J. E., Kimble, M., Hoyle, H. D., Subler, M. A. and Raff, E. C. (1987). Three Drosophila beta-tubulin sequences: a developmentally regulated isoform (ß3), the testis-specific isoform (ß2), and an assembly-defective mutation of the testis-specific isoform (B2t8) reveal both an ancient divergence in metazoan isotypes and structural constraints for beta-tubulin function. Mol. Cell. Biol. 7, 2231-2242.

Sagata, N., Shiokawa, K. and Yamana, K. (1980). A study on the steady-state population of Poly (A)+ RNA during early development of *Xenopus laevis*. Dev. Biol. 77, 431-448.

Sambrook, J., Fritsch, E. F. and Maniatis, T. (1989). Molecular cloning, a laboratory manual.(Nolan, C., Ed.). Cold Spring Harbor Laboratory Press, Cold Spring Harbor.

Schibler, M. J. and Huang, B. (1991). The col R4 and col R15 beta-tubulin mutations in *Clammydomonas reinhardtii* confer altered sensitivity to microtubule inhibitors and herbicides by enhancing microtubule stability. J. Cell Biol. 113, 605-614.

Scott, C. A., Walker, C. C., Neal, D. A., Harper, C. E., Bloodgood, R. A., Somers, K. D., Mills, S. E., Rebhun, L. I. and Levine, P. A. (1990). Beta-tubulin expression in normal and malignant epithelial cells. Arch. Otolaryngol., Head Neck Surg. 116, 583-589.

Scotto, K. W., Hildegard, K. and Roeder, R. G. (1989). Positive and negative regulation of the gene for Transcription Factor IIIA in *Xenopus laevis* oocytes. Genes Dev. 3, 651-662.

Serrano, L., de la Torre, J., Maccioni, R. B. and Avila, J. (1984). Involvement of the carboxyl-terminal domain of tubulin in the regulation of its assembly. Proc. Natl. Acad. Sci. USA 81, 5989-5993.

Skoufias, D. A., Burgess, T. L. and Wilson, L. (1990). Spatial and temporal colocalization of the golgi apparatus and microtubules rich in detyrosylated tubulin. J. Cell Biol. 111, 1929-1937.

Sobrier, M. L., Chapel, S., Couderc, J. L., Micard, D., Lecher, P., Somme-Martin, G. and Dastugue, B. (1989). 20-OH-ecdysone regulates 60C beta tubulin gene expression in Kc cells and during *Drosophila* development. Exp. Cell. Res. 184, 241-249.

Stearns, T., Evans, L. and Kirschner, M. (1991). Gamma-tubulin is a highly conserved component of the centrosome. Cell 65, 825-836.

Stein , R. and Ziff, E. B. (1984). HeLa cell beta-tubulin gene transcription is stimulated by adenovirus 5 in parallel with viral early genes by an E1a-dependent mechanism. Mol. Cell. Biol. 4, 2792-2891.

Sullivan, K., Lau, J. and Cleveland, D. (1985). Apparent gene conversion between beta-tubulin genes yields multiple regulatory pathways for a single beta-tubulin polypeptide isotype. Mol. Cell. Biol. 5, 2454-2465.

Sullivan, K. F. and Cleveland, D. W. (1986). Identification of conserved isotype-defining variable region sequences for four vertebrate ß-tubulin polypeptide classes. Proc. Natl. Acad. Sci. USA 83, 4327-4331.

Sullivan, K. F., Havercroft, J. C. and Cleveland, D. W. (1984). Primary structure and expression of a vertebrate beta-tubulin gene family. Mol. Biol. Cytoskel. 174, 321-332.

Sullivan, K. F., Havercroft, J. C., Machlin, P. S. and Cleveland, D. W. (1986a). Sequence and expression of the chicken ß5- and ß4-tubulin genes define a pair of divergent ß-tubulins with complementary patterns of expression. Mol. Cell. Biol. 6, 4409-4418.

Sullivan, K. F., Machlin, P. S., Ratrie, H. and Cleveland, D. W. (1986b). Sequence and expression of the chicken ß3 tubulin gene. J. Biol. Chem. 261, 13317-13322.

Swan, J. A. and Solomon, F. (1984). Reformation of the marginal band of avian erythrocytes in vitro using calf-brain tubulin: peripheral determinants of microtubule form. J. Cell Biol. 99, 2108-2113.

Theodorakis, N. G. and Cleveland, D. W. (1992). Physical evidence for cotranslational regulation of beta-tubulin mRNA degradation. Mol. Cell. Biol. 12, 791-799.

Thisse, B., Stoetzel, C., Gorostiza-Thisse, C. and Perrin-Schmitt, F. (1988). Sequence of the twist gene and nuclear location of its protein in endomesodermal cells of early *Drosophila* embryos. EMBO J 7, 2175-2183.

Vale, R. D. and Hotani, H. (1988). Formation of membrane networks by *in vitro* kinesin driven microtubule movement. J. Cell Biol. 107, 2233-2241.

Valenzuela, P., Quiroga, M., Zaldivar, J., Rutter, W. J., Kirschner, M. W. and Cleveland, D. W. (1981). Nucleotide and corresponding amino acid sequences encoded by alpha and beta tubulin mRNAs. Nature 289, 650-655.

Villasante, A., Wang, D., Dobner, P., Dolph, P., Lewis, S. A. and Cowan, N. J. (1986). Six mouse alpha-tubulin mRNAs encode five distinct isotypes: testis-specific expression of two sister genes.

Mol. Cell. Biol. 6, 2409-2419.

Wagner, A. P., Reck, G. and Platt, D. (1992). Dynamics of gene expression for microtubule-associated protein MAP1B, embryonic alpha-tubulin and late neural beta-tubulin mRNAs in the hippocampus of aged rats. Biochem. Biophys. Res. Comm. 184, 292-299.

Wang, D., Villasante, A., Lewis, S. A. and Cowan, N. J. (1986). The mammalian ß-tubulin repertoire: hematopoietic expression of a novel, heterologous ß-tubulin isotype. J. Cell Biol. 103, 1903-1910.

Webb, A. C. and Smith, L. D. (1977). Accumulation of mitochondrial DNA during oogenesis in *Xenopus laevis*. Dev. Biol. 56, 219-225.

White, R. A. H. and Wilcox, M. (1985). Distribution of Ultrabithorax proteins in *Drosophila*. EMBO J 4, 2035-2043.

Winning, R. S., Shea, L. J., Marcus, S. J. and Sargent, T. D. (1991). Developmental regulation of transcription factor AP2 during *Xenopus laevis* embryogenesis. Nuc. Acids Res. 19, 3709-3714.

Yen, T. J., Gay, D. A., Pachter, J. S. and Cleveland, D. W. (1988a). Autoregulated changes in stability of polyribosome-bound ß-tubulin mRNAs are specified by the first 13 translated nucleotides. Mol. Cell. Biol. 8, 1224-1235.

Yen, T. J., Machlin, P. S. and Cleveland, D. W. (1988b). Autoregulated instability of ß-tubulin mRNAs by recognition of the nascent amino terminus of ß-tubulin. Nature 334, 580-584.

Yisraeli, J. K., Sokol, S. and Melton, D. A. (1990). A two-step model for the localization of maternal mRNA in *Xenopus* oocytes: involvement of microtubules and microfilaments in the translocation and anchoring of Vg1 mRNA. Development 108, 289-298.

Zheng, Y., M.K., J. and Oakley, B. R. (1991). Gamma-tubulin is present in *Drosophila melanogaster* and *Homo sapiens* and is

associated with the centrosome. Cell 65, 817-823.